



Institut Supérieur de l'Aéronautique et de l'Espace

PIE-004

Very Low Altitude Mega Constellation

Authors and signature :

CAPANO Tommaso

CHAUVENT Louis

CHEVRIER Charles-Antoine

COULON Xavier

DOMINGO Marc

NDIAYE Issa

Supervisors :

ARMELLIN Roberto, ISAE

We hereby declare that this submission is our own work and to the best of our knowledge it contains no plagiarised material and all sources are correctly referenced and cited.

Version 1.0
October 22, 2020

Contents

| | | |
|----------|--|-----------|
| 1 | Summary | 4 |
| 2 | Introduction | 5 |
| 2.1 | Background and key issues | 5 |
| 2.2 | Contribution of this work | 5 |
| 2.2.1 | Mission analysis | 5 |
| 2.2.2 | Satellite preliminary design | 5 |
| 2.2.3 | System costs | 6 |
| 2.3 | Description of this report structure | 6 |
| 3 | Project management | 7 |
| 3.1 | Organisation | 7 |
| 3.2 | PBS | 9 |
| 3.3 | WBS | 10 |
| 3.4 | Gantt | 11 |
| 3.5 | Tracking Dashboard | 12 |
| 3.6 | Risks/opportunities | 13 |
| 4 | Technical report | 14 |
| 4.1 | Mission analysis | 14 |
| 4.1.1 | Constellation type and satellites coverage | 14 |
| 4.1.2 | Gateways sites | 17 |
| 4.1.3 | Launch vehicles assessment and selection, launch strategy | 20 |
| 4.1.4 | Reliability and spare management | 20 |
| 4.2 | Satellite, subsystems and budgets | 25 |
| 4.2.1 | Satellite configuration and external accommodation concept | 25 |
| 4.2.2 | Payload concept | 25 |
| 4.2.3 | Propulsion concept and budget - assessment of air breathing propulsion alternative | 27 |
| 4.2.4 | ADCS concept | 30 |
| 4.2.5 | Power concept and budget | 32 |
| 4.2.6 | Thermal subsystem | 33 |
| 4.2.7 | Mass budget | 34 |
| 4.3 | Systems cost | 34 |
| 4.3.1 | CAPEX (capital expenditure) | 34 |

| | |
|--|-----------|
| 4.3.2 OPEX (operational expenditure) | 35 |
| 5 Conclusion | 36 |
| 5.1 Reliability | 37 |
| 5.2 Constellation type and satellites coverage | 37 |
| 5.3 Optimal number of Gateways | 60 |
| 5.4 Reliability and spare management | 62 |
| 5.5 ADCS concept | 72 |

1 Summary

Very low altitude mega constellation with thousands of satellites are a new opportunity to provide low latency connectivity services with a global coverage service.

Several projects with similar purpose already exist such as the OneWeb or Starlink constellation. Using very low earth orbit is interesting in many aspects : so called "self cleaning" orbits (no debris issue), less power is required to close the link budget, and the environment have a low radiation level, allowing the use of COTS components.

Nevertheless, more satellites are required to fully cover the Earth, hence requiring more gateways sites. In addition, the atmospheric drag is a critical issue at low altitude.

First the design of the constellation and gateways is performed in order to reduce the overall system cost. Once the constellation and gateways are obtained, a unique satellite design is done to reduce the costs. Launch vehicle options is assessed along with the satellite design to optimize its shape. A study about system reliability and spare management is also performed.

Even with the air breathing propulsion alternative, it was found that lowest altitudes are not optimal. A preliminary design of constellation, gateways and satellites is provided and justified, while respecting the specified constraints.

Key words : *satellite constellation, Low Earth Orbit, satellite concept, mission analysis, air breathing*

2 Introduction

2.1 Background and key issues

The space system studied is a very low altitude mega constellation of satellites, with thousands of satellites in order to provide low latency connectivity services with a global coverage service. The mission purpose is similar to OneWeb or Starlink constellations but operated from a very low altitude (between 200 and 400 km). Such mega constellation in LEO (Low Earth Orbit) enable a faster communication than with usual geostationary satellite, which would be an asset for financial businesses, e.g. trading where low latency is critical, and for entertainment purposes, e.g. gaming where low latency is required to provide a seamless and smooth experience to the user.

The main advantages of the very low altitude is that there is no debris issue (so-called "self cleaning" orbits), smaller payloads require less power to close the link budget, resulting in smaller satellites. As the satellites are smaller, more satellites can be launched at once. The LEO environment have a low radiation level, allowing the use of COTS components. However more satellites are needed to provide a full Earth coverage, requiring more gateways sites. Moreover the issue of atmospheric drag must be handled with care.

2.2 Contribution of this work

The work done in the PIE is to do a preliminary design of such a very low altitude mega constellation. Three main parts can be identified, mission analysis, satellite preliminary design and the estimation of system costs.

2.2.1 Mission analysis

- Constellation type and satellites coverage
- Amount of gateways sites
- Candidate launch vehicles assessment and selection
- Orbit selection and constellation sizing
- Hot and cold spares strategy to ensure quality of service

2.2.2 Satellite preliminary design

- Perform satellite functional analysis and establish simplified satellite functional architecture
- Establish preliminary satellite configuration concept (antennas, solar arrays, radiators, sensors, thrusters....)
- Estimate atmospheric drag, derive propulsion requirements and select candidate propulsion systems

- Assess air breathing propulsion alternative
- Assess antenna concept for user & feeder links and user beams layout
- Size telecommunication payload and establish simplified architecture
- Investigate required attitude and navigation sensors and actuators
- Perform preliminary power subsystem sizing
- Establish power & energy, mass and propellant budgets
- Establish preliminary 3D external accommodation concept

2.2.3 System costs

The system cost need to be estimated, in particular the CAPEX (capital expenditure) and the OPEX (operational expenditure). The CAPEX consist of the cost of satellites, launches and gateways whereas the OPEX is related to the cost of operations (control of the constellation from the ground, gateway operations, ...).

2.3 Description of this report structure

This report is organised in five main sections : a 200 words summary, this introduction, a section about the project management, a section describing the technical solutions proposed and how they where obtained, and finally a conclusion opening to potential new work and improvement on the subject.

The technical solutions are described in three parts : mission analysis, satellite, subsystems and budgets, and system costs.

3 Project management

The project is developed along four main lines of progress in parallel in order to integrate the results obtained over time:

- Constellation sizing and orbit selection
- Analysis of the aerothermodynamic environment and design of the propulsion system
- Functional analysis of the satellite with mass, power and energy budgets
- Payload design and telecommunication system

Each of these analyses requires information and details from the results of the others. Hence, it is not possible to perform these tasks independently. Therefore, the development was based on an iterative process where the models were constantly refined.

The analyses conducted individually were therefore followed by a weekly meeting to update the models, review the different work packages and share the results obtained.

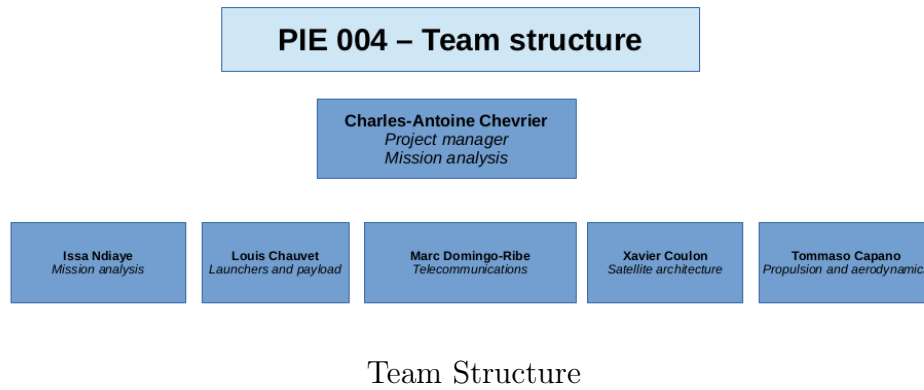
To better manage resources, a role is assigned to each person in the team, which corresponds to key points in the Project. Subsection 3.1 lists the main roles of each team member. Moreover, a responsibility assignment matrix is used to better explain the roles and responsibilities in cross-functional tasks.

From 3.2 to 3.5 the organization of the project is presented in terms of how the project is divided, tasks assignation, the required time for each task and the evolution of the project in time. Finally in 3.6 the risks and opportunities of the project are presented.

3.1 Organisation

Each role was assigned to each team member based on their skills and preferences. The technical specialization of each team member had a heavy impact on the assignment of roles. However, the motivation of each individual to chose another task that has nothing to do with his specialization was considered too.

We defined roles linked to the main stones of the project. Figure below shows how the team is organized.



To have a better management of the project and work more efficiently a responsibility assignment matrix is defined. This matrix relates the responsibilities of each one of the team in relation to the different sub-tasks into which the project is divided.

Four levels of responsibility has been defined:

- **R - Responsible:** The one who realizes
- **A - Accountable:** The one who supervises and reports
- **I - Consulted:** The one who advises
- **C - Informed:** The one who is informed

| | Sous-tâches | IN | LC | MD | XC | CAC | TC |
|--|----------------|-----|-----|-----|------|-----|-----|
| Analyse Mission | 1.1.1 à 1.1.5 | RAI | I | I | I | RI | I |
| Lanceurs | 1.1.6 | I | RAI | I | RI | I | I |
| Stratégie spares & fiabilité | 1.1.7-1.1.8 | I | RAI | I | I | I | I |
| Télécommunications - charge utile | 1.2.5 à 1.2.6 | I | I | RAI | I | I | I |
| Propulsion, aérodynamisme | 1.2.2 à 1.2.4 | I | I | I | I | I | RAI |
| Architecture Satellite | 1.2 | I | I | I | RAI | I | RI |
| Coûts | 1.3.1 et 1.3.2 | IC | IC | IC | RAIC | IC | IC |
| Chef de Projet | 1.4.1 et 1.4.2 | I | I | I | I | RAI | I |

Responsibility assignment matrix: **IS:** Issa Ndiaye, **LC:** Louis Chauvet, **MD:** Marc Domingo, **XC:** Xavier Coulon, **CAC:** Charles-Antoine Chevrier, **TC:** Tommaso Capano

3.2 PBS

The PBS provides a hierarchical structure of the things that the project will make or outcomes that it will deliver. This project will deliver as a product the definition of a constellation and the gateways distribution that will provide a specific type of service. Moreover, a first sizing of the satellite is delivered. Hence, the PBS Figure below shows the main parts of the satellite with the specific subsystems that has to be defined and sized.

This project will also deliver the CAPEX and the OPEX of the whole system. Moreover, a spare management to achieve the client requirements and the assessment of the launching options (fairing capacity, cost...) are delivered too.

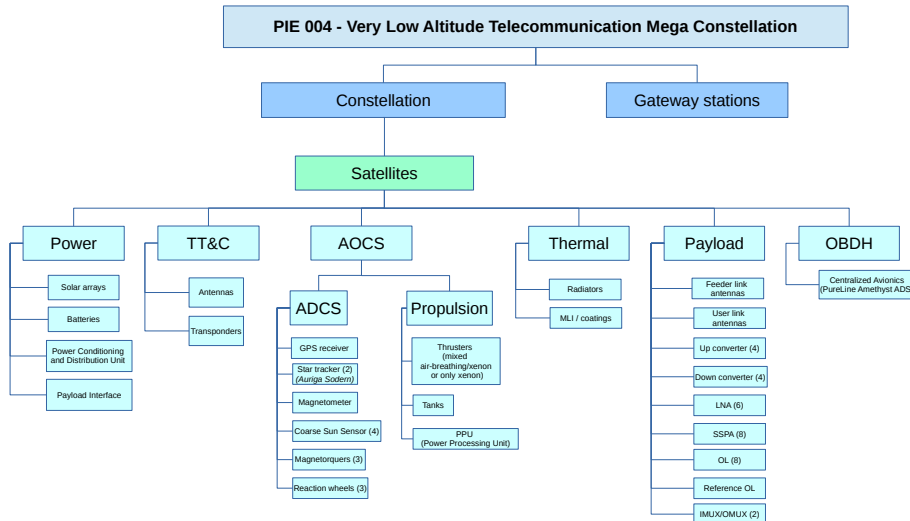


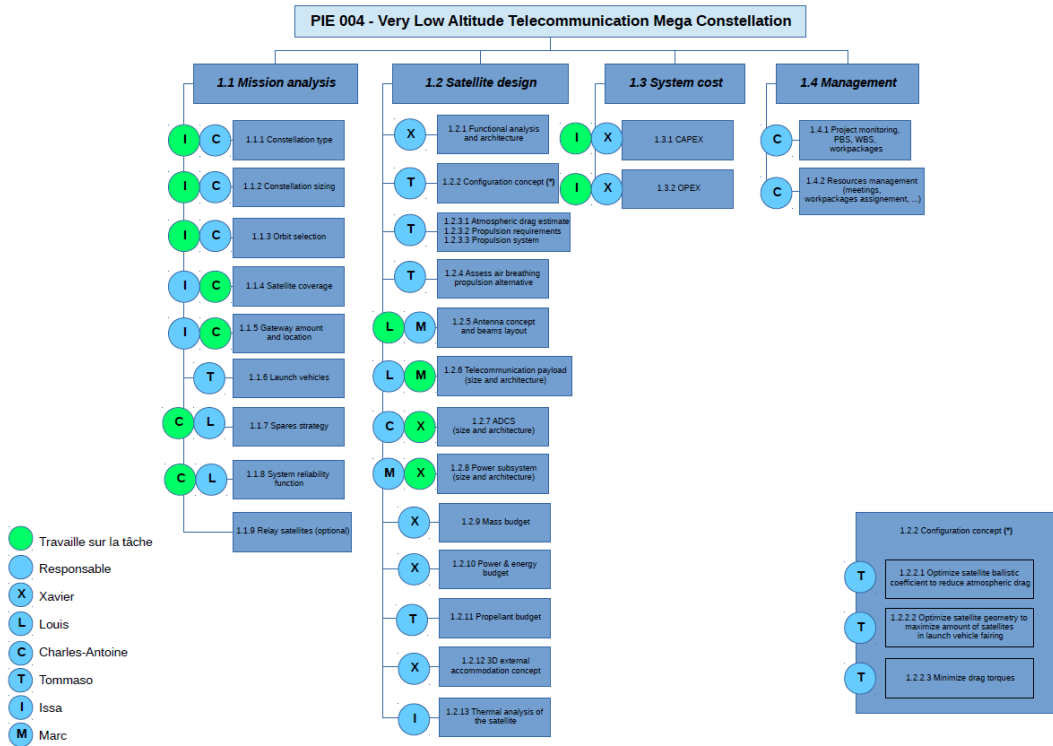
Figure 1: PBS: Product Breakdown Structure

3.3 WBS

The WBS is a deliverable-oriented breakdown of a project into smaller components. This is used to organize the team's work into manageable sections. This project is divided in four main tasks:

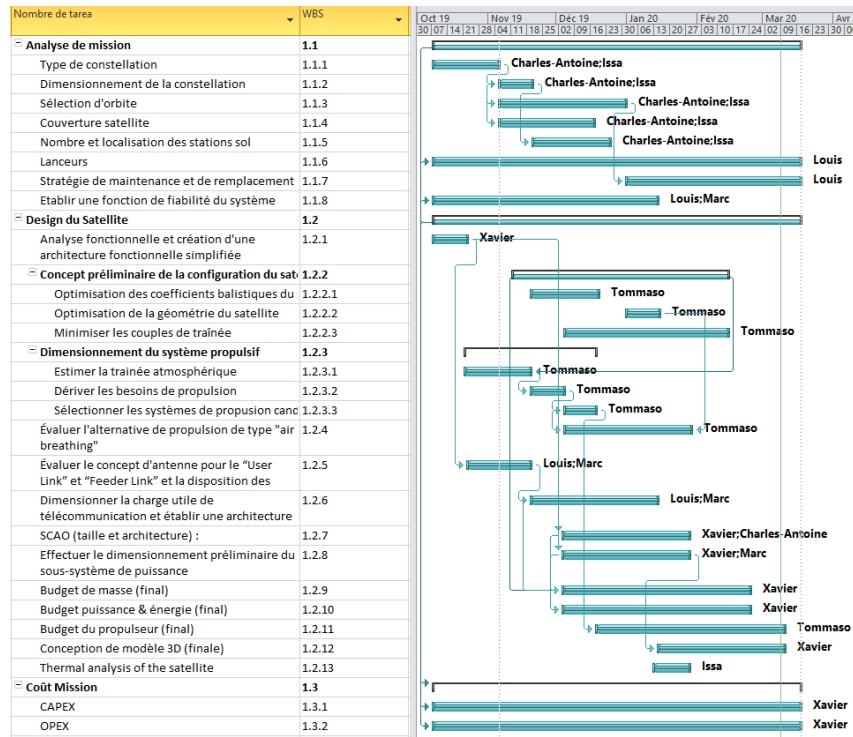
- Mission Analysis (Constellation design, Spare management, Launch management and Gateway)
- Satellite design
- System Cost (OPEX, CAPEX)
- Project management

Each task is divided into sub-tasks to organize better the team and reach the aim of the main task quicker and more efficiently. Each task and subtask are labeled with a number to better monitor the project evolution with the Gantt. Moreover, the WBS shows the team members assigned to each task and also the grade of responsibility of these members to that task.



3.4 Gantt

The Gantt chart illustrates the project schedule. Each task and sub-task are labeled with a number for a better monitoring. The Gantt below shows the start date and end date of each task/sub-task of the project. Moreover, it shows the dependency between sub-tasks and the one in charge of each sub-task.



The Gantt is modified as the project advances. Some tasks have to be extended in time due to setbacks. Others had to be reduced in time as they were oversized. Moreover, the Gantt provides an estimation of the number of hours that each team member will work. In this project we estimated 80h of work per team member.

The table below shows the estimated number of hours and the real number of hours for each team member. A precise count was not performed but estimated by each member every month.

| Member | Estimated Hours | Real Hours |
|---------------------------------|-----------------|------------|
| Charles-Antoine Chevrier | 80 | 95 |
| Issa Ndiaye | 80 | 90 |
| Louis Chauvet | 80 | 87 |
| Marc Domingo | 80 | 85 |
| Xavier Coulon | 80 | 88 |
| Tommaso Capano | 80 | 90 |

All the team members exceeded the estimated hours due to unexpected complications or details that were not considered.

3.5 Tracking Dashboard

The monitoring dashboard includes a date-date table, as well as the main characteristics of the elements to be sized (choice of orbits, etc...). The dashboard was updated at each project team meeting with the client (every 2 weeks). A meeting report was written during each of these meetings.

The Figure below shows some delay in some tasks during the development of the project. This was particularly due to poor time management as some team members were overloaded with work, explaining the drift in time, for example for the propulsion tasks. A proper rescheduling of the task and external help solved the issue.

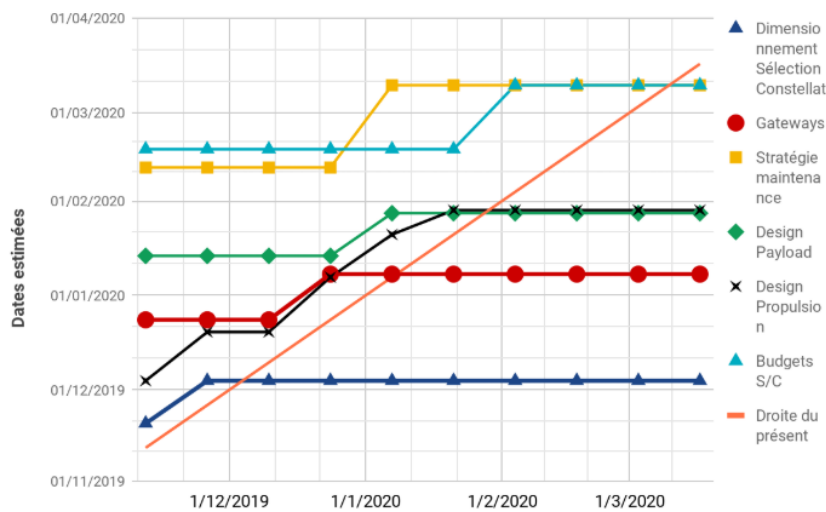


Figure 2: Date-date table

3.6 Risks/opportunities

A table of the possible risks during the development of the project is defined to predict the uncertainties in the project and minimize the occurrence or impact of these uncertainties. The table below summarises the Cause, Event and Consequence that can impact negatively the project.

| Num | Category | Cause (fact) | Risk Event | Consequence |
|-----|-----------|---|-------------------------|----------------------------|
| 1 | Technical | Crash of Google servers (Drive) / Error of manipulation | Loss of data | Project Delay/Cancellation |
| 2 | Technical | Customer communication problem | Deliverable Discrepancy | No customer satisfaction |
| 3 | Technical | Limitation of team competence | Study lock | Delay/Incomplete study |
| 4 | Technical | Unavailability ressource | Resource unavailability | Delay/Incomplete study |
| 5 | Technical | Poor planification | Poor planning | Delay |
| 6 | Human | Injury/illness of a team member | Inability of a member | Delay on the deliverable |

Table 1: Risks description

Once the risks are defined, preventive actions to reduce the risk events are considered. The table below shows the impact when a risk event occurs and its probability before and after the preventive actions are considered.

| Num | Pre-response Assesment | | Risk Response | Post-response Assesment | | |
|-----|------------------------|--------|---|-------------------------|--------|----------|
| | Proba | Impact | | Probability | Impact | Score |
| 1 | 1,00E-05 | Critic | Regular data recording | 1,00E-07 | Major | 1,00E-06 |
| 2 | 1,00E-02 | Major | Bimonthly progress meetings | 1,00E-05 | Minor | 1,00E-05 |
| 3 | 1,00E-03 | Minor | Self-study/teacher assistance | 1,00E-03 | Minor | 1,00E-03 |
| 4 | 1,00E-03 | Minor | Reassigning tasks / Reassessing the schedule | 1,00E-03 | Minor | 1,00E-03 |
| 5 | 1,00E-01 | Major | Project management meetings and meetings with supervisors | 1,00E-03 | Minor | 1,00E-03 |
| 6 | 1,00E-02 | Major | Member Replacement Plan | 1,00E-02 | Minor | 1,00E-02 |

Table 2: Risk impact before and after response assessment

The opportunities that will provide us this project are to expand the knowledge through the project and the advice/support of the technical advisor and teachers we contact.

4 Technical report

4.1 Mission analysis

4.1.1 Constellation type and satellites coverage

Constellation type assessment

According to the requirements, a complete and continuous coverage is necessary. In order to assess the coverage and characteristics of each constellation type, some angles are defined, see annexe 5.2.

Four configurations are discussed here, table 3. Notice that for each constellation, the inclination and altitude of the satellites is the same for all planes, except for the last strategy where there is an altitude plane separation. It appears that the Walker Delta constellation is not optimal and it is discarded for the Walker Star constellation containing less planes than the Walker Delta. The use of rectangular footprint allows to have planes with a different orbital speed, removing the phasing between planes issue. In addition, the plane altitude separation feature reduces the collision probability between planes, which is an interesting feature regarding the number of satellites involved in the constellation.

- Walker Delta constellation (circular footprint) [3] (same inclination and altitude for all planes)
- Walker Star constellation or "Streets of coverage" constellation [3] (circular footprint), section 5.2 (same inclination and altitude for all planes)
- Rectangular footprint constellation, (same inclination and altitude for all planes)
- Rectangular footprint constellation with plane altitude separation, (same inclination for all planes)

| | Advantages | Drawbacks |
|--|---|--|
| Walker Delta (circular footprint) ("Streets of coverage") [3] | Simple and academic design | - Requires twice as many planes than Walker Star - Requires a correct phasing between adjacent planes |
| Walker Star (circular footprint) [3] | Simple and academic design | Requires a correct phasing between adjacent planes |
| Rectangular footprint | No superposition of footprint required | User beam layout not trivial |
| Rectangular footprint with plane altitude separation | - Different orbital speed (hence altitude) can be used for each plane - Lower collision probability between planes | Interference can appear at the border of each footprint (each plane as a different orbital speed) |

Table 3: Summary of the different constellation types assessed

An analysis with analytical derivations to design the different constellation types is performed in annexe 5.2 and Matlab script are used to generate the constellation characteristics. A description of the different constellation can be found in annexe 5.2.

Analysis of the cost to optimize the constellation design

Two different costs functions are used : a simple cost function and an advanced cost function.

Simple cost function

The simple cost function is a function of the number of satellites that need to be built, the number of planes directly related to the number of launches, the number of Gateways to be built and the number of antennas to be used per Gateway (which depends on the number of satellites seen from the Gateway, hence depends on the Gateway latitude).

$$\text{cost} = 0.25 * \text{NbSat} + 50 * \text{ceil}\left(\frac{\text{NbSatPlane}}{100}\right) \text{NbPlane} + f(\text{Gateway}, \text{Antennas}) \quad (1)$$

It is assumed that the cost of one satellite is 0.25 M€, a launch 50 M€ and that each launch can carry 100 satellites. Of course each of these figures has an influence on the conclusions, especially the number of satellites that can be launched at once.

Advanced cost function

An advanced cost function is designed on the basis on some data given by our technical supervisor. A fit is done on the data to obtain different functions : the launch vehicle capacity LVCapacity with respect to the altitude chosen for the launch, the mass of the satellite SatMass with respect to the altitude and the cost of one satellite SatCost with respect to the altitude. The satellite mass and cost are computed with the 5 years lifetime scenario. After having computed the number of planes and number of satellites per plane required to obtain the constellation, the mass and cost of each satellite is computed and the maximum value is selected for the cost function. Indeed one must keep in mind that all the satellites should be exactly the same, therefore the worst case should be used to size to system. The number of launches required is computed for each plane, i.e. for each altitude, thanks to the total mass of the satellites on a plane to be launched and the launch vehicle capability. A factor of 15% is added to the total mass of the satellites in order to take the adaptor mass into account. The cost of a launch is still assumed to be 50 M€.

$$\text{cost} = \text{SatCost} * \text{NbSat} + 50 * \text{ceil}\left(\frac{\text{NbSatPlane} * \text{SatMass}}{\text{LVCapacity}}\right) \text{NbPlane} + f(\text{Gateway}, \text{Antennas}) \quad (2)$$

Notice that there is an altitude constraint imposed by the ISS : the upper limit for the altitude is chosen to be 388 km (see annexe for full discussion). The degrees of freedom for the different constellation configurations are listed in the table 4 :

| | Walker Star | Rectangular footprint | Rectangular footprint (altitude plane separation) |
|---|--------------------|------------------------------|--|
| Altitude | x | x | x (initial altitude) |
| Inclination | x | x | x |
| Spacing | x | | |
| Length/Width ratio <i>OR</i> Number of S/C per plane | | x | x |
| Altitude separation between planes | | | x |

Table 4: Different degrees of freedom for the design of the constellation

Results of the optimisation

All the different figures mentionned in this discussion are displayed in annexe 5.2. Additional comments can also be found in annexe 5.2.

Basically the number of planes and satellites per planes decreases when the altitude increases therefore the best altitude to reduce the number of planes and satellites would be the highest, Figure 28. An inclination closer to 90° reduces also the number of planes requires to cover the business latitude $\pm 70^\circ$. The spacing parameter in the Walker Star constellation and the ratio between length and width or fixed number of satellites per plane show non trivial optimum and plateaus (corresponding to a new plane).

The rectangular footprint constellation with plane altitude separation is selected for its properties reducing collision and removing the need of in-phase planes. The inclination selected is polar, 90° of inclination and the altitude separation between two planes is fixed at 1 km (loss of altitude after 10 orbits at 300 km).

The figures 42 to 53 describe the cost with respect to the initial altitude and the length to width ratio or the number of Satellites per plane show different features :

- the cost is smaller for higher altitudes
- some plateaus can be identified and the overall look of the cost function is in stairs due to the discrete values of the problem (number of satellites, number of planes)

Some pixels are blank : either it is because the ISS constraint is not fulfilled (all the satellites should be at altitudes lower than 400 km) or the problem is unfeasible (not enough satellites per plane to cover the whole plane). The simple cost analysis shows that the best is always to go the highest possible to minimise the cost, Figure 44 to 46 and Figure 50 to 51.

Without the ISS constraint, there is an optimum with the advanced cost function that appears Figure 48 and 52. However with the ISS constraint the optimum are at the border of the admissible set, Figure 49 and 53. Notice that for the simple cost the optimum is already at the border of the admissible set, at the highest initial altitude possible (here the maximal initial altitude tested is 400 km).

Final configuration selected

The optimal solutions are reported table 15 and 14. The final configuration selected, which is optimal with regard to the constraints and costs defined, is described below :

| | Rectangular footprint Constellation Plane Altitude Separation |
|---|---|
| 1 | Satellites : 6400 |
| 2 | Number of planes : 40 |
| 3 | Inclination : 90 deg |
| 4 | Elevation min : 50 deg |
| 5 | Altitude from : 347.7 km to 386.7 km, equally spaced by 1 km |
| 6 | Mode : 0 (0:fixed NbSatPlan, 1:fixed Footprint Ratio) |
| 7 | Fixed number of satellites per plane : 160 |

4.1.2 Gateways sites

Number of Gateway estimated with the paper [2]

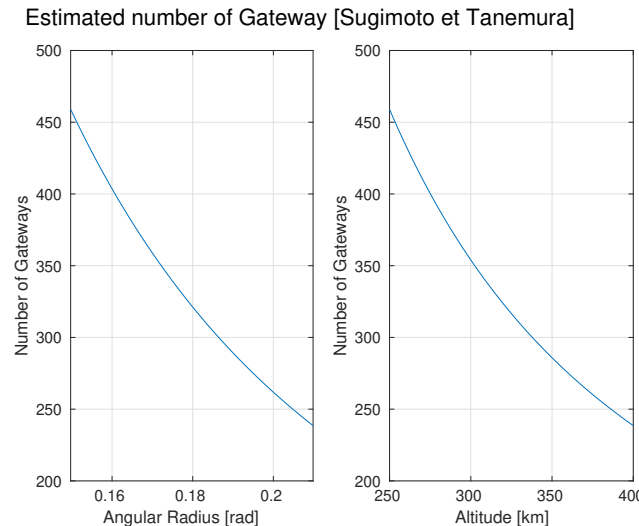


Figure 3: Number of gateways with respect with the angular radius [rad] and altitude [km] [2]

The number of gateways with respect with the angular radius [rad] and altitude [km] is given by [2], Figure 3.

Algorithm placing gateways

We use an algorithm inspired by Walker constellation that puts gateways along lines of equal latitudes :

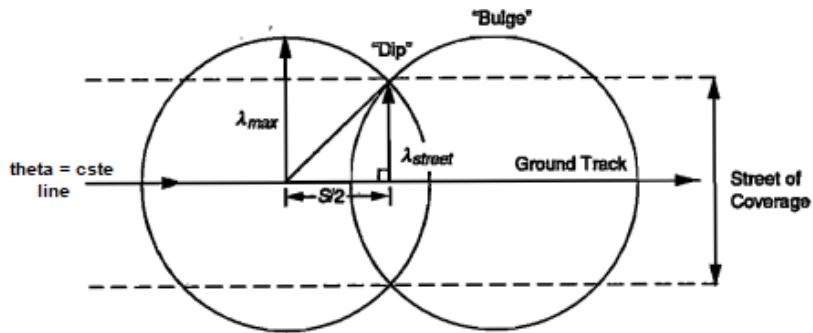


Fig. 7-10. The "Street of Coverage" is a Swath Centered on the Ground Track for which there is Continuous Coverage.

Figure 4: Street of coverage and coverage in adjacent latitudes

Using the distance on a sphere formula , with θ as the longitude and ϕ as the latitude : $D = \cos^{-1}(\cos(\theta_1)\cos(\theta_2)\cos(\Delta\phi) + \sin(\theta_1)\sin(\theta_2))$

$$\cos(\lambda) = \cos(\theta)\cos(\theta + \lambda_{street})\cos\left(\frac{\lambda_s}{2}\right) + \sin(\theta)\sin(\theta + \lambda_{street})$$

$$(1) : A\cos(x) + B\sin(x) = C \text{ with } \begin{cases} x = \theta + \lambda_{street} \\ A = \cos(\theta)\cos\left(\frac{\lambda_s}{2}\right) \\ B = \sin(\theta) \\ C = \cos(\lambda) \end{cases}$$

We solve it with $t = \tan\left(\frac{x}{2}\right) \implies (1) : A(1 - t^2) + 2Bt = C(1 + t^2)$

Finally, we will find 2 different λ_{Street} , as :

$$\lambda_{Street} = 2 * \tan^{-1}(t) - \theta \text{ with } (A + C)t^2 - 2Bt + (C - A) = 0$$

Which gives 2 solutions :

A positive λ which corresponds to the North width of coverage.

A negative λ which corresponds to the South width of coverage.

The spacing between gateways on each latitude row is a parameter, we know that :

-If the spacing is the same between two rows, we can go back to a Walker type case and separate the latitudes by $\lambda + \lambda_{street}$.

-If the spacing is different, we need to use the equations and consider $\lambda_{street1} + \lambda_{street2}$.

Once we optimized these parameters and perfected by hand the optimization, the solution found is :

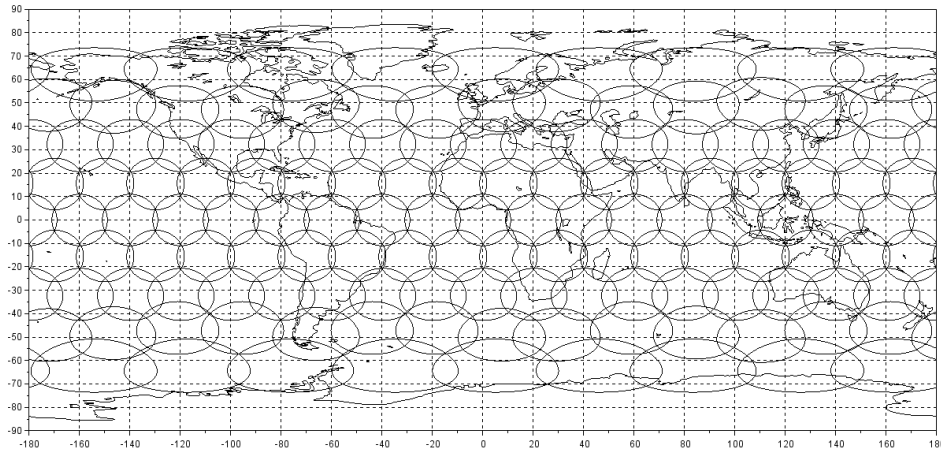


Figure 5: Ground track visibility (minimum elevation 10°)

Here we have 136 gateways for an altitude of 350km.

Number of antennas needed

We need to calculate how many satellites can be reached by a gateway depending on its latitude. To do this, a simple matlab algorithm based on the position of all satellite can compute the maximum number of satellites reached by the gateway.

| Latitude(degree) | 0 | 16 | 32 | 48 | 61 |
|---|----|----|----|----|----|
| Maximum number of active satellites seen | 52 | 51 | 56 | 67 | 46 |

Table 5: Satellites reached by gateways depending on their latitude

For an initial altitude of 350km, 136 Gateways and 7465 antennas are needed.

Gateways positions

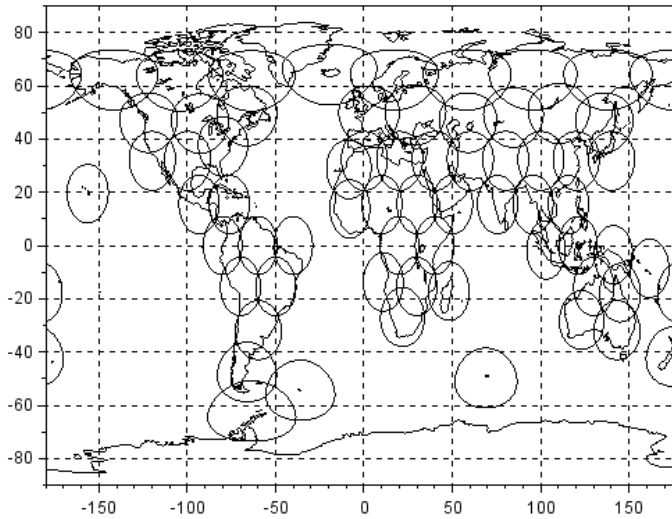


Figure 6: Ground track visibility (minimum elevation 10°)

When we adjust for the land : 66 Gateways and 3600 Antennas.

4.1.3 Launch vehicles assessment and selection, launch strategy

The selected launchers to put the constellation in orbit are two: Ariane 6 by Ariane Group and SpaceX's Falcon 9 (fig. 7). This is due to their convenient cost per launch and the size of their fairing that easily fit the spacecraft to be accommodated in. The launch strategy is such that a single rocket will put in orbit all the spacecraft of a single plane; this is considered the best trade-off between the number of launches to be done, the rockets' payload mass and the in-space maneuvers to be done to position all the spacecrafts in their operative slot. Concerning their disposition inside the fairing, the satellites will be clamped around 4 hexagonal supports, each of them providing dispenser to carry 8 layers of 6 satellites each, as shown in figure 8. It gives a total 192 spacecraft to fit into a fairing, enough to cover an orbital plane.

4.1.4 Reliability and spare management

Reliability

Each satellite is designed with a constant failure rate $\lambda(t) = \lambda$ and has therefore a reliability (probability of survival from time 0 to t) given by : $R(t) = e^{-\lambda t}$.

Thus the probability of having a satellite failure within a duration t of operation is given by $p_{fail}(t) = 1 - R(t) = 1 - e^{-\frac{t}{MTBF}}$ with the Mean Time Between Failures

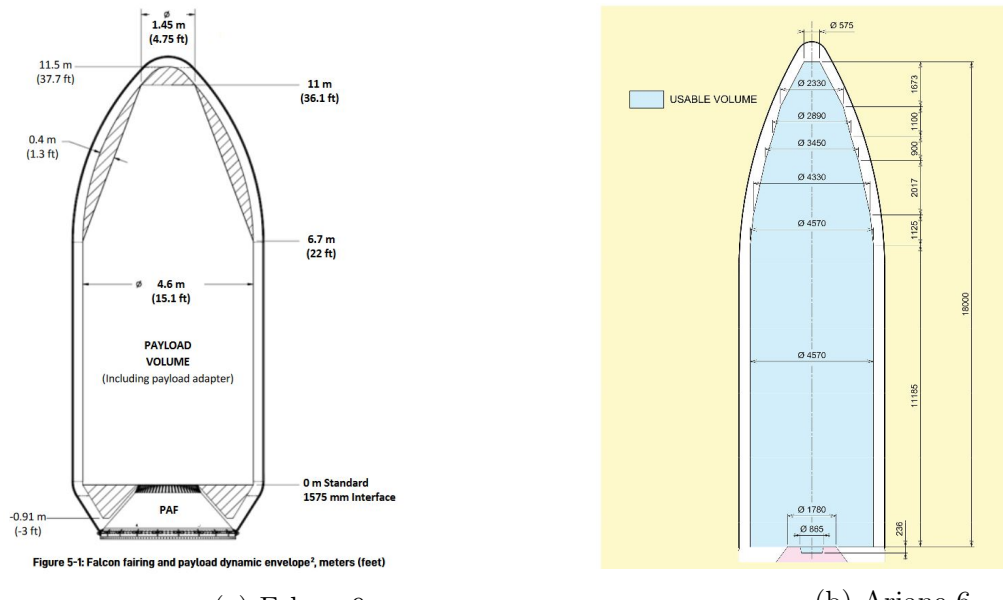


Figure 7: Rocket fairings selected to put the constellation in orbit

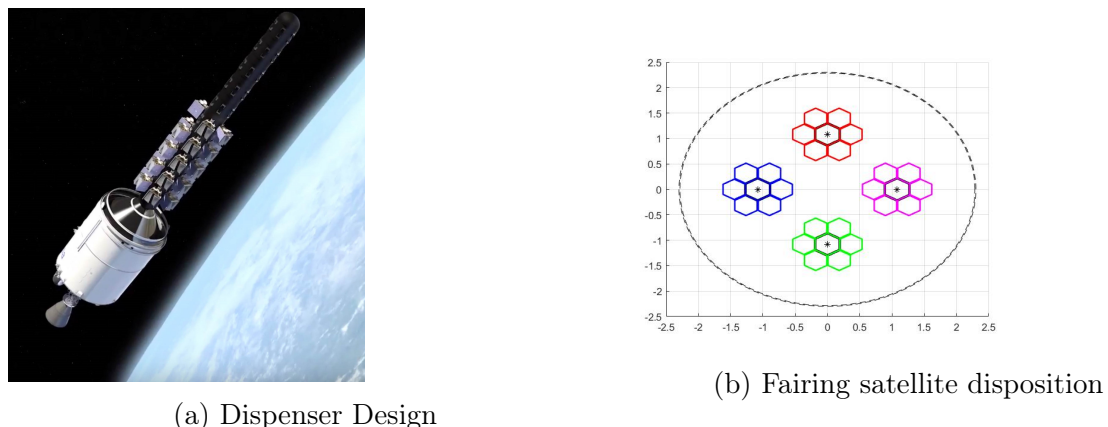


Figure 8: Satellites disposition concept inside the fairing

$MTBF = \frac{1}{\lambda}$. After a time $U = 5$ years which is the designed satellite maximum lifetime the probability of survival is 0.

With given values of the reliability of one satellite after 5 years of operation, the failure rates have been calculated at different temperature of the equipment as shown in Table 6 and the reliability over time is plotted on Figure 9.

| Temperature (°C) | Reliability after 5 years | Failure Rate (h^{-1}) | MTBF (years) | MTTR (days) |
|------------------|---------------------------|---------------------------|--------------|-------------|
| 0 | 0.9 | $2.41 \cdot 10^{-6}$ | 47.46 | 87.04 |
| 10 | 0.88 | $2.92 \cdot 10^{-6}$ | 39.11 | 71.74 |
| 20 | 0.85 | $3.71 \cdot 10^{-6}$ | 30.77 | 56.43 |
| 30 | 0.81 | $4.81 \cdot 10^{-6}$ | 27.73 | 43.52 |
| 40 | 0.76 | $6.27 \cdot 10^{-6}$ | 18.22 | 33.42 |

Table 6: Failure rates values given reliabilities at the end of mission at different temperatures

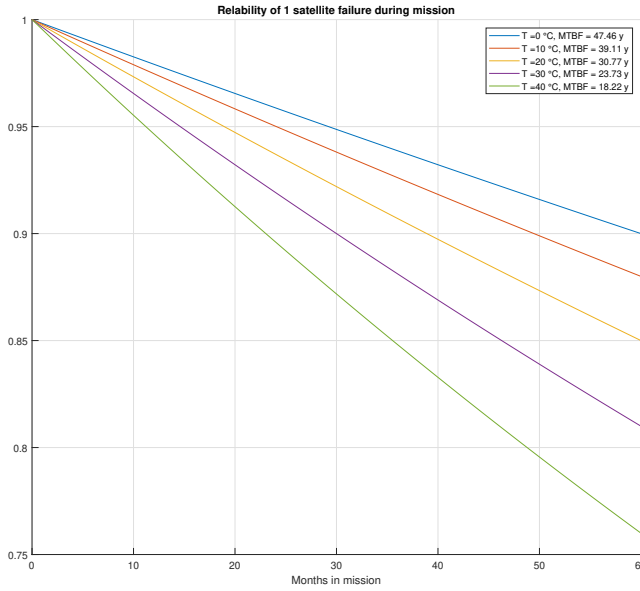


Figure 9: Reliability of one satellite

For a given user the maximum time of visibility of one satellite T_{vis} is given by:

$$T_{vis} = T_{orb} \frac{\psi}{180}$$

with T_{orb} the period of one orbit and ψ the angle of the cone corresponding to the coverage of one satellite (depending on the elevation $\epsilon = 50^\circ$ and the altitude of the satellite). In the worst scenario of having a user crossing of the coverage of the same defective satellite twice in 24 hours, the time ratio of having service in one day is:

$$\rho = 1 - \frac{2T_{vis}}{24h}$$

The worst case scenario of having multiple satellite failures is when a user is seeing all of the faulty satellites one after the other. It has been calculated that a user sees 7 or 8 satellites of the same plane before seeing ones of the next plane. Hence the worst configuration of satellite failures is a longitudinal one as seen in Figure 10.

It has been showed that the probability of having failures in this configuration only depends on the total number of satellite in the constellation and is highly unlikely [4]. Therefore we will assume randomly distributed occurring failures in the whole constellation.

The requirements specify a quality of service of $\rho_{min} = 99.5\%$, it gives a maximum number k_{max} of failures acceptable for continuously

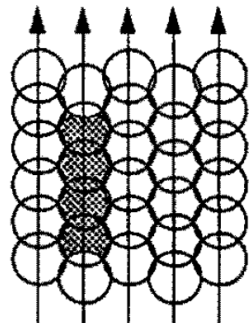


Figure 10: Longitudinal configuration of failures [4]

delivering this quality of service.

$$k_{max} = \lfloor \frac{24h}{2T_{vis}}(1 - \rho_{min}) \rfloor$$

Computing these formulas, with the highest plane at 386.7 km and the required quality of service of 99.5% (applying the ratio of emerged ground), gives a maximum time of visibility of $T_{vis} = 82.04$ s and a maximum of $k_{max} = 8$ satellites failures at the same time.

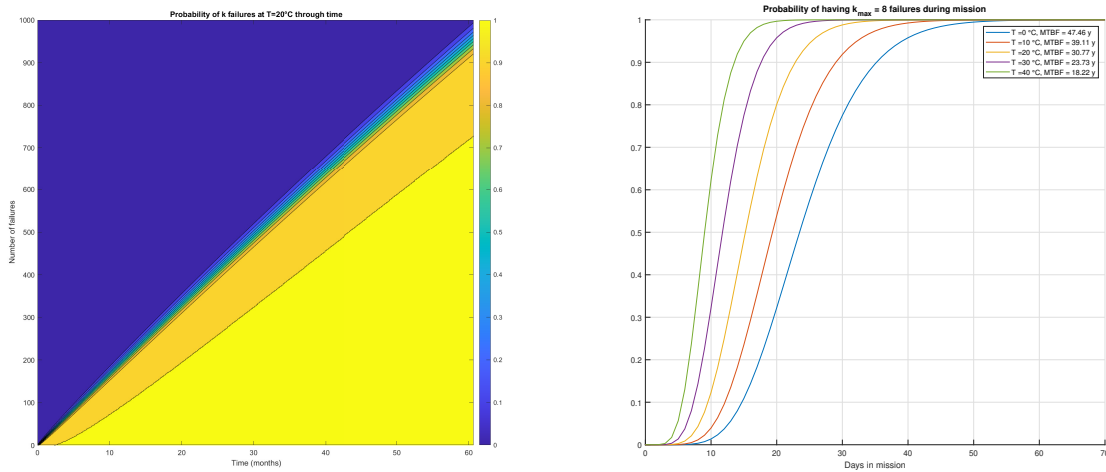
The probability of having a least k satellite failures given a probability $p_{fail}(t)$ of failure after a period t follows a Binomial distribution with $N = 6400$ satellites :

$$p_k(t) = 1 - \sum_{i=0}^{k-1} \binom{N}{i} p_{fail}(t)^i (1 - p_{fail}(t))^{N-i} = \sum_{i=k}^N \binom{N}{i} p_{fail}(t)^i (1 - p_{fail}(t))^{N-i}$$

$$R_{sys}(t) = \mathbb{P}(n_{fails} < k_{max} = 8)(t) = \sum_{i=0}^7 \binom{N}{i} p_{fail}(t)^i (1 - p_{fail}(t))^{N-i}$$

$$\text{MTBF}_{sys} = \int_0^\infty R_{sys}(t) dt = \int_0^\infty \sum_{i=0}^7 \binom{N}{i} (1 - e^{-\frac{t}{\text{MTBF}}})^i e^{-\frac{(N-i)t}{\text{MTBF}}} dt = \frac{\text{MTBF}}{120} F(N, k_{max})$$

These probabilities over time are shown on Figure 11, having this many satellites results in reaching the maximum of failures by 20 to 50 days of mission. It means that it is needed to have between 300 and 800 more satellites depending on the temperature through 5 years of mission to be able to compensate the failures.



(a) Probability of having at least k failures through time at $T = 20^\circ C$ (b) Probability of having at least $k_{max} = 8$ failures through time at $T = 20^\circ C$

Figure 11: Probabilities of satellite failure over time

Spare management

Three different strategies are investigated in order to deal with the spares, see details annexe 5.4 :

- Oversizing the payload or equivalently using more active satellites per plane than needed such that a certain number of satellites can fail without an outage of service. After a certain number of failures, a new batch is launched from the ground.
- In plane idle spares : the time for a failed satellite to be repaired is directly the time needed to rephase correctly the plane where the satellite failed. After a certain number of failures, a new batch is launched from the ground.
- Above planes of spares : one or several planes are above the ISS with an inclination smaller than 90° in order to use the RAAN drift to catch up with the plane where the failed satellite is.

Comparison and tradeoff

For all the strategies, about the same number of spare satellites are launched : it is exactly the same cost for the first and second strategy, the satellites are injected in the nominal orbits, however for the last strategy (above planes) the satellites need to be put in a higher orbit. Notice that for the first and second strategy it is possible to add the spares to the nominal launches so that no extra launch is required (or a few ones only). For the last strategy it is required to have extra launches, at least 4 as 4 planes are chosen for this strategy.

For one failure, all the satellites need to be properly phased for the first and second strategy whereas for the above planes strategy the spare is inserted directly in the proper position. (Notice that the failed satellite needs to be removed from the position before, by natural decay or thanks to telecommand).

The cost and time related to the maneuvers shows that the first and second strategy are faster and consume less fuel than the last one. However one should keep in mind that for the last strategy less or no fuel is consumed to fight the atmospheric drag. The hazards encountered during maneuvers are also different for the different strategies. A more detailed analysis can be found in annex. All this discussion is summed up table 7.

With the different characteristics of each strategy, the best one seems to be the hot spares strategy, where one satellite position can be replaced in 3 to 4 days :

- It can be launched with the nominal batches
- The cost of maneuvers is reduced compared to the above plane strategy

| | Hot spares | Idle spares (one man.) | Idle spares (several man.) | 4 planes |
|-------------------------------------|-----------------------|-------------------------------|-----------------------------------|-----------------|
| Launches | With nominal launches | With nominal launches | With nominal launches | >4 |
| S/C maneuvers | N-2 | 1 | $\frac{N_0}{2N}$ | 1 |
| Total duration | 3-4 days | >80 days | 5-6 days | / |
| Cost (ΔV) | 0,5 m/s | 0,5 m/s | 0,5 m/s | >3 km/s |
| Cost (mass) | 4.2 g | 4.2 g | 4.2 g | >22.5 kg |
| S/C state | nominal mode | mission idle, thrust on | mission idle, thrust on | idle |

Table 7: Comparison of the different strategies (continuous thrust durations)

4.2 Satellite, subsystems and budgets

4.2.1 Satellite configuration and external accommodation concept

One main challenge for the satellite concept would be the accommodation. Indeed, in order to reduce the cost and optimize the launch, the satellite must be as small and compact as possible. This raised the issue of the accommodation, every subsystem need to be place on-board and organize them is an important task. Moreover the low orbit compel us to have a small front surface in order to reduce the atmospheric drag.

Taking into consideration both the atmospheric drag issue and the launch strategy, the following design have been selected.

The hexagonal shape allows to maximize the number of satellite per launch and minimize the front surface.

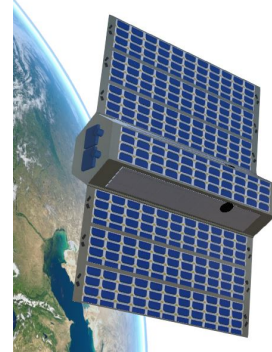


Figure 12: External accommodation concept

4.2.2 Payload concept

The main functions of the telecommunication payload are to receive and transmit carriers over a frequency band from (and to) earth gateways or user terminals. The satellites will be regeneratives, meaning there will be no processing on board (transparent payload) and will use multibeam antennas for an optimal use of the frequency band and for a significant boost in capacity.

The convention of the telecommunication links is defined on the Figure 13a and as the frequency plan by the Table 8.

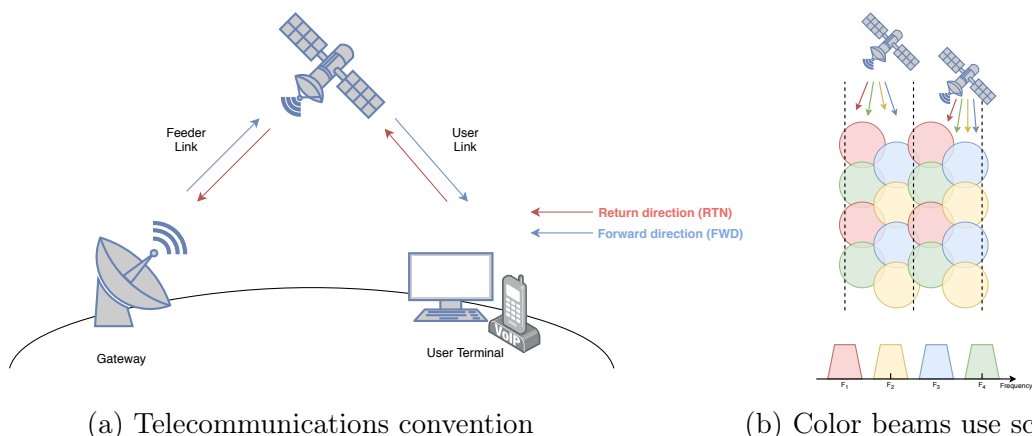


Figure 13: Telecommunication multibeam concept

The communications payload transmitters and receivers consist in multiple antennas to have a four colors frequency scheme as seen in Figure 13b. We will use the same antennas for the Tx and Rx for the user link and two sets (Tx and Rx) of two same antennas

| | GHz | Channel 1 | Channel 2 | Channel 3 | Channel 4 |
|------------|--------------------|-----------------|-----------------|-----------------|-----------------|
| FWD | Feeder link | [27.50 – 27.96] | [28.07 – 28.53] | [28.64 – 29.10] | [29.50 – 29.96] |
| | User link | [10.70 – 11.16] | [11.21 – 11.67] | [11.73 – 12.19] | [12.24 – 12.70] |
| RTN | User link | [14.00 – 14.12] | [14.13 – 14.25] | [14.25 – 14.37] | [14.38 – 14.50] |
| | Feeder link | [17.80 – 17.93] | [18.02 – 18.15] | [18.25 – 18.38] | [18.47 – 18.60] |

Table 8: Frequency plan table

for the feeder link.

Two sets of antennas (Rx and Tx) are needed for the feeder link because we need to be able to switch gateways without lowering our quality of service requirements of 99.95%, so the second antenna will manage the gateway handover. For the user link we will use 4 antennas, one for each color beam.

The payload will consist firstly in a Low Noise Amplifier (LNA) which has a high gain (around 40 dB) which is needed in order to minimise noise contribution when going through the next element of the payload which is the Down Converter (Up Converter for the RTN direction). The converter is mixer with a local oscillator which translates the frequency of the signals to meet the requirements of the Table 8 (for the FWD we need to go from Ka to Ku band and the opposite for the RTN direction). We then combine our 4 parallel channels together with an IMUX (OMUX decomposition for the FWD direction) before amplifying the signal with two SSPAs, very high gain amplifiers in order to reach the desired RF power of the budget link. The telecommunication payload is shown on Figure 14.

We will put three spares of LNA and U/C converters for each direction between the four original ones, then one spare of SSPA for each direction also.

As previously mentioned 4 fixed antennas are used for the user link, one per each channel. These antennas are used to transmit and receive the information. The type of antenna used in the user link is a simple dual band patch antenna of 8dB of Gain. The UL antennas are placed at the nadir of the satellite with an inclination of 21° to provide the correct beam distribution to provide service to all users included in the field of visibility of the satellite. The feeder link differently to the UL uses mobile antennas to provide the link with the gateways. Moreover, two sets of Tx/Rx pairs are used to manage the gateway handover. The antenna type selected for the TX and the RX is a patch array antenna that provides 22dB of Gain. To provide a reliable link the platform that supports each set of Tx/Rx antennas has the capacity to tilt the antennas 70° in each direction.

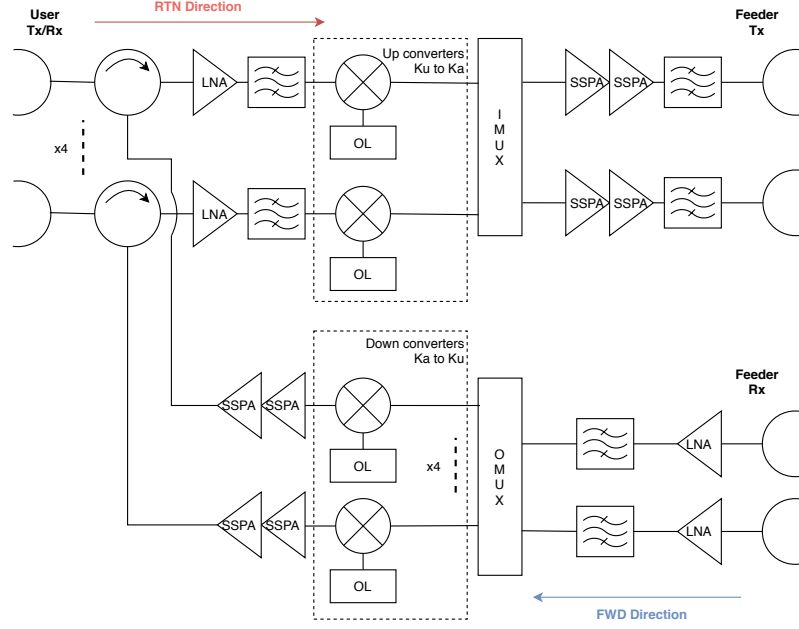


Figure 14: Telecommunications payload (without redundancy)

4.2.3 Propulsion concept and budget - assessment of air breathing propulsion alternative

Drag Coefficient estimation

The whole constellation will operate in a LEO environment. A major issue for orbits belonging to this class is the need for compensation of Drag forces and torques induced by the residual presence of gas particles. It is thus crucial to correctly estimate the aerodynamical properties of the satellite in order to evaluate its performances. The two key parameters to determine are the drag coefficient c_D and the cross section area A_{cross} that have a primary influence on the resulting drag.

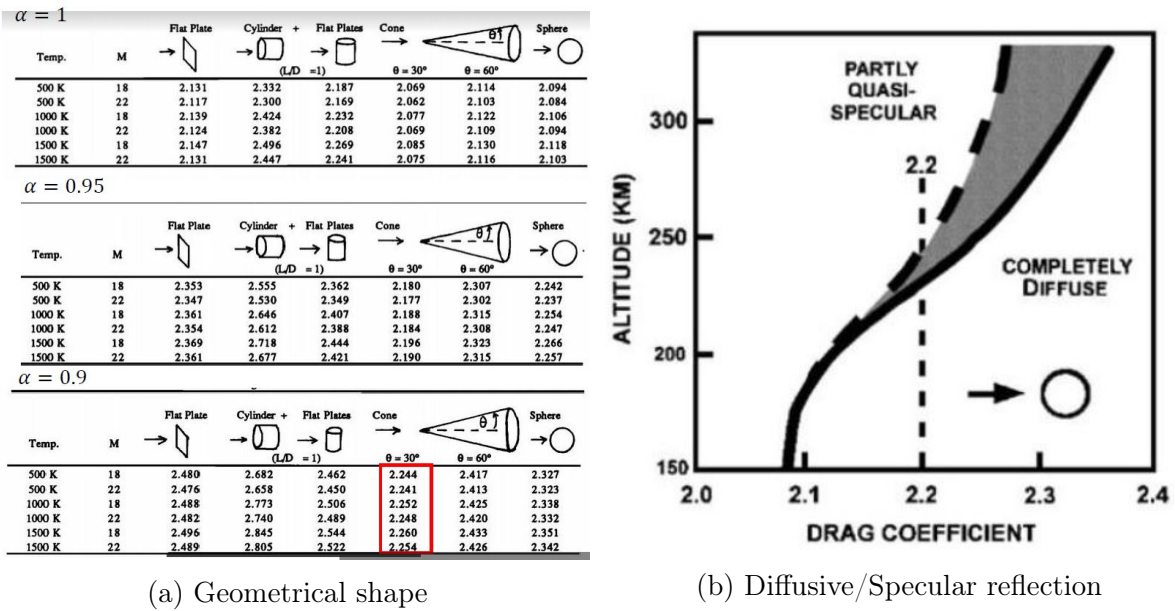


Figure 15: Drag coefficient estimation according to the geometry and physical model considered

Figure 16 shows the results of analysis conducted for a series of shapes to estimate the associated drag coefficient. The reference surface considered is the cross-wet section of the spacecraft in order to eliminate the dependence on any geometrical variation along the longitudinal axis. Also, analytical models are available to determine the numerical value of c_D starting from the analysis of molecules impact on the surface. It can be seen in figure 15b that if scattering phenomena are taken into account, the drag coefficient will be affected consequently. According to these result, one can conclude that, for a given section A_{cross} , the drag coefficient value can be bounded by its maximum value obtainable, $c_{D,Max} = 2.5$, and that its average value is around 2.2.

In the following paragraphs a value of $c_D = 2.5$ in order to be conservatives; this choice in fact introduces margins that can compensate some model uncertainties.

Atmospheric density and Drag

The environment selected for the constellation varies from $200Km$ to $400Km$ in altitude. As it can be seen in figure 16a, the atmosphere density profile is smooth with the altitude, taking values ranging from $\rho_{max}(h = 200) = 10^{-10}Kg/m^3$ to $\rho_{min}(h = 400) = 10^{-13}Kg/m^3$ in the considered interval. Also, it should be noticed that the density is strictly dependent on the solar activity: this introduces some oscillations that can be as big as an order of magnitude and whose period is equal to a solar cycle (that is, 11 years approximately). Since the constellation is designed to operate continuously to provide the service, satellites must be capable of operating nominally even in worse case conditions (maximum solar activity). However, it would be too conservative to consider the maximal solar activity as a sizing condition, since no satellite would experience this condition for his whole lifetime. Thus, an average condition was taken between minimal and maximal solar activity (dashed line in figure).

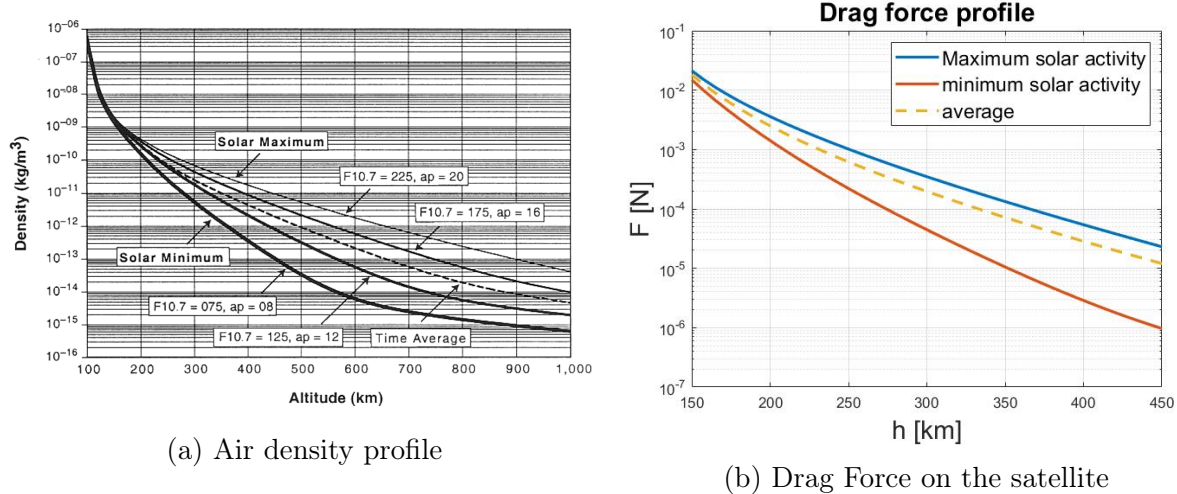


Figure 16

Starting from the density profile, to obtain the drag force acting on the spacecraft, the following parameters were taken:

- the cross section is the one of a circle with a radius of 20 cm: $A_{cross} = \pi 0.2^2$;
- the orbit is circular and polar: $e = 0$, $i = 90^\circ$, $v = \sqrt{\frac{\mu_E}{h}}$
- the density is an average condition between minimal and maximal solar activity;

The results are given in figure 16b. It can be seen that the order of magnitude can range from $10^{-3}N$ to $10^{-5}N$ approximately. This means that, a priori, every group of satellite orbiting on the same plane should be equipped with a specific engine to optimise its performances. However, this would be extremely inconvenient from a design viewpoint since every spacecraft would be different from the ones of another planes. Thus, a limit case would be taken considering the lowest altitude of the constellation, that is $h_{min} = 350Km$. The rest of the satellite will be then oversized with respect to their optimal design in terms of propulsion.

Air Breathing Propulsion system

The altitude range considered for the constellation is such that the drag is continuously active, tending to slow down the satellite. An interesting option to consider is to use the incoming airflow to generate thrust, thus eliminating the need for a propellant tank to load on-board. It follows that a conspicuous save in weight can be achieved. The concept is currently under development and is known as *Air Breathing Technology*. Concerning the state of the art, ESA recently announced that a first prototype was created and tested managing to ignite and burn using only air at orbital densities. However, it is not clear yet if this system was able to compensate for the resulting drag or not. It can be assumed though that the technological readiness level will be reached by the time the constellation will be launched, also considering potential economical investments that could be made specifically for the present case.

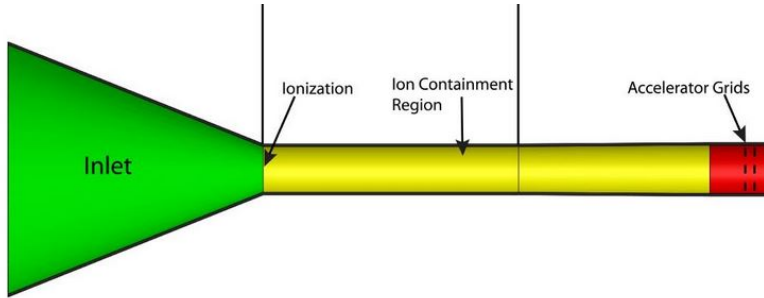


Figure 17: Air Breathing Engine Technology

A schematic representation of the engine is shown in figure 17. It consists of an inlet acting as a collector for the incoming air, a ionisation module that generates plasma, an ion confinement duct and the grid acceleration, where the propellant is ejected. Despite the interest and the numerous advantages that this solution could offer, it was eventually decided not to chose it for the following reasons:

- the ionisation process is based on microwave discharge. The technology is already existing and operative, however the ionisation efficiency drastically decreases at low densities. This physical limit may be overcomes in future years but it is hard to provide reliable estimations for this value;
- The inlet material should be at the same time light and particularly resisting to corrosion due to the high presence of mono-atomic oxygen. Studies are being conducted but this could be a limiting factor for long term missions as the present one;
- The optimal range in altitude is actually higher than the domain of interest for an *Air Breathing Engine*. Researches in fact are focusing rather on orbits of 200 km about.

Hall Effect Thruster

A more classical solution is given by an electrical engine that uses Xenon as a propellant. The drawback of storing liquid fuel into the satellite is actually compensated by a lighter engine. The specific impulse considered is $I_{sp} = 1200$ s. The performances were calculated considering an average density profile to size the tank and the mass of propellant to store. The power and thrust capabilities were instead obtained considering the worst case scenario (that is, maximum solar activity) and adding the possibility to perform an extra maneuver in case of failure of a nearby satellite. The selected engine features a power of 20 W, generating a maximum thrust of 0.2 mN. The Xenon to be stored is approximately 3 kg heavy, giving an overall weight of 4.14 kg.

4.2.4 ADCS concept

Different components are selected in order to provide a proper attitude and position estimate and to actuate the satellite. Details about each component can be found in

annexe 5.5.

| Component/Mode | Detumbling/LEOP | Mission | Desaturation | Safe |
|--------------------------|-----------------|---------|--------------|------|
| GNSS receiver (1) | x | x | x | x |
| Star trackers (2) | | x | x | |
| Coarse Sun Sensors (3/4) | x | x | x | x |
| Magnetometer (1) | x | x | x | x |
| Magnetorquer (3) | x | | x | x |
| Reaction wheels (3) | | x | | |

Table 9: ADCS architecture and modes

Several modes can be identified during the life of the spacecraft :

- Detumbling/LEOP : the satellite uses the Earth magnetic field and magnetorquers to stabilize the satellite after the initial launch thanks to a B-dot law. Notice that the thrusters are not used during this very first phase.
- Mission mode : the reaction wheels are used to provide a good pointing while dealing with the torques generated by the environment and the thrust. The star trackers are also used to provide a precise attitude.
- Desaturation mode : the reaction wheels are used in a regenerative breaking mode, i.e. some energy is recovered thanks to the breaking and the magnetorquers are used to desaturate the wheels.
- Safe mode : only the coarse sun sensors and magnetometer are used to obtain a rough estimate of the Sun position for the Sun acquisition to retrieve power from the Sun.

The ADCS strategy is to use the reaction wheels between $\pm 70^\circ$ of latitude (maintaining a precise attitude over business areas) and then to off-load the reaction wheels thanks to the magnetorquers above the poles. Additional off-loading might also be performed above the sea and non business regions.

The star tracker chosen for the mission is Auriga by Sodern, which is also used for the OneWeb constellation, hence well suited for our project (uses COTS, good balance between performance and mass/power). Two star trackers with pointing direction separated by 70° are enough to ensure attitude estimation all the time. A study was done (cf annexe 5.5) to check that the sensors are not blinded during the mission (notice that Auriga is not blinded by the Moon). The ADCS architecture does not contain gyroscope, as two star trackers are enough to provide an estimate of the attitude. A gyroscope will add complexity and increase the cost of the system, therefore it was chosen to not use a gyroscope. The sizing of the reaction wheels and the magnetorquers is detailed in annexe 5.5. The different results of the sizing are displayed table 10 and 11. The sizing was based on the analysis of the external and internal torques.

| Momentum storage | Maximum torque | Mass | Size | Power |
|------------------|----------------|-------|-------------------------------|------------|
| 0.2 N.m.s | >0.1 mN.m | 500 g | 100 mm diameter, 48 mm height | cf Fig. 67 |

Table 10: Reaction wheel design

| Magnetic moment | Mass | Size | Power |
|--------------------|------|-----------------------|-------|
| 12 Am ² | 470 | Φ=12 mm, length=85 mm | 3 W |

Table 11: Magnetorquer design

4.2.5 Power concept and budget

Power budget

This power budget aims to estimate the power consumption of all on-board systems in order to sizing both the solar array subsystem and the battery. Power subsystem sizing task describes the power system selection and sizing considerations for our satellite. A preliminary analysis is use to size component power, based on mission parameters.

In order to sizing the power subsystem, a first power budget need to be established for a worst case scenario. This scenario correspond to a use of every subsystem (payload, propulsion, ADCS...) at its maximal power consumption. This mode is only use as a sizing mode and do not correspond to a real mode of the satellite.

| ▼ System modes | | | ↑↓ | * | * | * | * | * |
|--|-------------------|---|-----------|------------------|----------------------|--------------------------|-----------------------------|--------------------|
| | | | | SAFE | MISSION | DESATURATION | DETUMBLING-LEOP | SIZING |
| | | | | System mode SAFE | System mode MISSION | System mode DESATURATION | System mode DETUMBLING-LEOP | System mode SIZING |
| ▼ Platform | | | | | | | | |
| + | Subsystem | + | Equipment | Instance | Element Mode > | Custom | Element mode NOMINAL | Element mode MAX |
| ► | Subsystem PROP | | | | Without margin [W] | 8,5 | 8,5 | 8,5 |
| | | | | | Including margin [W] | 8,5 | 8,5 | 8,5 |
| ► | Subsystem ADCS | | | | Without margin [W] | 3,54 | 29,59 | 29,59 |
| | | | | | Including margin [W] | 3,54 | 29,59 | 29,59 |
| ► | Subsystem ELEC | | | | Without margin [W] | 18 | 18 | 18 |
| | | | | | Including margin [W] | 18 | 18 | 18 |
| ► | Subsystem TMTC | | | | Without margin [W] | 5,3 | 5,3 | 5,3 |
| | | | | | Including margin [W] | 5,3 | 5,3 | 5,3 |
| Consumed power without margin | | | | | 35,34 | 61,39 | 61,39 | 36,39 |
| Consumed power including margin | | | | | 35,34 | 61,39 | 61,39 | 36,39 |
| Consumed system power margin | | | | | 0,00% | 0 | 0 | 0 |
| Total consumed power including system margin | | | | | 35,34 | 61,39 | 61,39 | 36,39 |
| ▼ Payload | | | | | | | | |
| + | Subsystem | + | Equipment | Instance | Element Mode > | Element mode OFF | Element mode MAX | Element mode OFF |
| ► | Subsystem PAYLOAD | | | | Without margin [W] | 0 | 52,1 | 0 |
| | | | | | Including margin [W] | 0 | 52,1 | 0 |
| ► | Subsystem PAYLOAD | | | | Without margin [W] | 0 | 52,1 | 0 |
| | | | | | Including margin [W] | 0 | 52,1 | 0 |
| Consumed power without margin | | | | | 0 | 52,1 | 0 | 52,1 |
| Consumed power including margin | | | | | 0 | 52,1 | 0 | 52,1 |
| Consumed system power margin | | | | | 0,00% | 0 | 0 | 0 |
| Total consumed power including system margin | | | | | 0 | 52,1 | 0 | 52,1 |
| Duty cycle | | | | | 0,00% | 0,00% | 0,00% | 0,00% |
| Total consumed power without any margin | | | | | 35,34 | 113,49 | 61,39 | 36,39 |
| Total consumed power without system margins | | | | | 35,34 | 113,49 | 61,39 | 36,39 |
| Total consumed system power margin | | | | | 0 | 0 | 0 | 0 |
| Total consumed power including system margins | | | | | 35,34 | 113,49 | 61,39 | 36,39 |

Figure 18: Power budget

Detail power budget (about each components) can be found in annexe.

Power subsystem sizing

The preliminary power budget give the instant consumption in the satellite. By taking in account different efficiencies and some power sizing rules, such as depth of discharge requirement or aging, we can estimate the battery's mass. Then, using orbit parameters, the surface of solar array needed can be estimate too.

4.2.6 Thermal subsystem

The thermal subsystem can be studied with the SYSTEMA software and its extension "Thermica". We modelized the mission in the software.

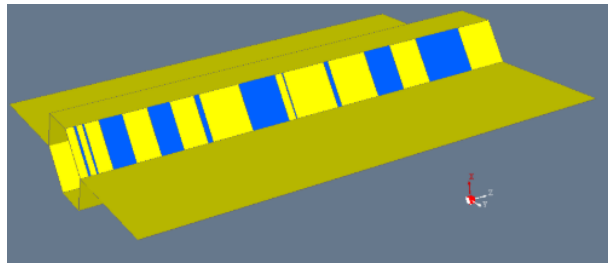


Figure 19: Satellite model

The best design for the radiators is :

- Symmetrical : The satellites will be exposed to the Earth and Sun in every angle.
- On the upper faces : The solar panels will move and overshadow the down faces, which makes big differences of radiations exposure between different satellites.

Consequently : the radiators will be placed on both right and left upper faces of the satellite.

We also need to consider all orbits in regards to the Sun (exposure and eclipse) to estimated the design.



Figure 20: Orbit examples

Finally, the computation made us reach a total radiator surface of 0.35m^2 .

4.2.7 Mass budget

This mass budget aims to estimate the final mass of the satellite. Monitoring the mass is very important for several reasons : - one of the client requirement is that the total mass of the satellite is less than 100 kg. - a smaller mass implies less cost during the launch

| Platform | | | | Target wet mass [Kg] : 50 | | Without margin [Kg] | Margin [%] | Margin [Kg] | Including margin [Kg] | % of total |
|--|------|----------|-----------|------------------------------|---------------|---------------------|---------------|--------------|-----------------------|--------------|
| + Subsystem | Name | Quantity | Mass [Kg] | Margin [%] | Forced values | Mass [Kg] | Margin [%] | | | |
| ► Subsystem STR | | | | | | 13,00 | 20,00% | 2,60 | 15,60 | 23,72% |
| ► Subsystem PWR | | | | | | 10,00 | 20,00% | 2,00 | 12,00 | 18,24% |
| ► Subsystem THERM | | | | | | 0,24 | 20,00% | 0,05 | 0,29 | 0,44% |
| ► Subsystem PROP | | | | | | 8,60 | 20,00% | 1,72 | 10,32 | 15,68% |
| ► Subsystem ADCS | | | | | | 3,96 | 20,00% | 0,79 | 4,75 | 7,22% |
| ► Subsystem ELEC | | | | | | 5,50 | 20,00% | 1,10 | 6,60 | 10,03% |
| ► Subsystem TMTC | | | | | | 0,20 | 20,00% | 0,04 | 0,24 | 0,36% |
| Total dry mass without system margin | | | | | | 41,50 | 20,00% | 8,30 | 49,79 | |
| System margin | | | | | | | | 0,00% | 0,00 | 49,79 |
| Propellant mass | | | | | | | | 0,00% | 0,00 | 0,00 |
| Total wet mass including all margins | | | | | | | | | 49,79 | |
| Payload | | | | Target wet mass [Kg] : 15 | | Without margin [Kg] | Margin [%] | Margin [Kg] | Including margin [Kg] | % of total |
| + Subsystem | Name | Quantity | Mass [Kg] | Margin [%] | Forced values | Mass [Kg] | Margin [%] | | | |
| ► Subsystem PAYLOAD | | | | | | 13,32 | 20,00% | 2,66 | 15,98 | 24,30% |
| Total dry mass without system margin | | | | | | 13,32 | 20,00% | 2,66 | 15,98 | |
| System margin | | | | | | | | 0,00% | 0,00 | 15,98 |
| Total wet mass including all margins | | | | | | | | | 15,98 | |
| System | | | | Target wet mass [Kg] : 65,78 | | Without margin [Kg] | Margin [%] | Margin [Kg] | Including margin [Kg] | % of total |
| Total dry mass without system margins | | | | | | | | | | |
| Total dry mass including system margins | | | | | | 54,81 | | 10,96 | 65,78 | |
| Total propellant mass | | | | | | 0,00 | 0,00% | 0,00 | 0,00 | |
| Total wet mass including all margins | | | | | | | | | 65,78 | |

Figure 21: Mass budget

Detail mass budget (about each components) can be found in annex.

4.3 Systems cost

4.3.1 CAPEX (capital expenditure)

Launch cost

As mentioned before (section 4.1.3), the optimal strategy selected is to fill an orbital plane with single launch; the overall number of launches to be done to put the whole constellation in orbit is therefore equal to the overall number of orbital planes, that is 60. Of course, it can be seen from table 12 that Falcon 9 gives a priori the cheapest solution in terms of costs, since by adopting a reusable core the price for a launch is almost half of that of competitors. However, availability and reliability factors should be taken into account, not to mention the fact that SpaceX is an American society; because of this, the Ariane 6 also represent a valid solution to be considered.

| Launcher | N°launches | Cost/launch | Tot. Cost |
|----------|------------|-------------|-----------|
| Ariane 6 | 40 | 70M€ | 2.8 B€ |
| Falcon 9 | 40 | 27M€ | 1.1 B€ |

Table 12: Launch costs for the two options selected

Satellites and Gateways cost

We use the cost estimation given to us by our technical supervisor Mr.Tourneur :

- Satellite : 1 M€
- Gateways : 5 M€
- Antennas : 0.1 M€

| Element | N°elements | Cost/launch |
|-----------|------------|-------------|
| Satellite | 6400 | 6.4B€ |
| Gateway | 66 | 0.33B€ |
| Antenna | 3600 | 0.36B€ |

Table 13: Satellite and Gateways Costs

The final CAPEX cost is estimated at 8.2 – 9.9 B€.

4.3.2 OPEX (operational expenditure)

The operation cost still needs to be estimated precisely.

Our first idea of estimation is based on the Galileo and Iridium constellations OPEX costs which are respectively 0.8B€, and 0.56B\$.

5 Conclusion

The results of this study contain the major aspects of mission analysis. The constellation type and design were optimized thanks to a cost function defined thanks to prior knowledge, as well as the number of position of gateway stations on the ground. The launching options were assessed : the fairing volume and overall cost of the launches were used to choose the best fit for the mission. The reliability of the system was considered and estimated to design a spare management strategy in order to ensure the service provided by the system within the requirements. The satellite design of the constellation was done knowing the worst cases of orbit, enabling to size the different subsystems (payload, ADCS, power subsystem, propulsion, ...). The system cost was also considered thanks to the OPEX and CAPEX that was used in particular to choose the constellation features by an optimisation process.

All in all this work provide a first sizing of a very low altitude mega constellation for telecommunication purposes, with a clear rationale about the different features selected.

This is of course a very first sizing which should be investigated more in details, with more simulations and more insights about the different components of the spacecraft.

5.1 Reliability

5.2 Constellation type and satellites coverage

Analytical derivations to design the constellation

Angle definitions

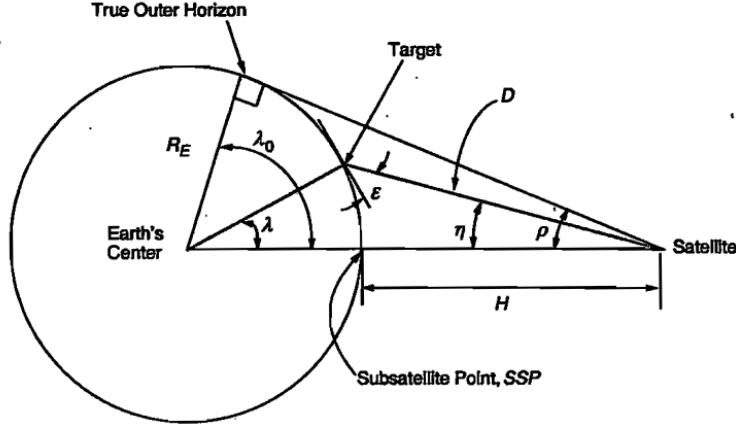


Figure 22: Definition of angular relationships between satellite, target, and Earth centre [1], p113

First the Earth central angle λ is computed with respect to the grazing angle or spacecraft elevation angle $\varepsilon=50^\circ$ and the satellite altitude H , Figure 22. The angular radius of the Earth ρ is obtained thanks to :

$$\sin \rho = \cos \lambda_0 = \frac{R_E}{R_E + H} \quad (3)$$

Then the nadir angle η is obtained :

$$\sin \eta = \cos \varepsilon \sin \rho \quad (4)$$

Thanks to the trigonometric relation $\lambda = 90^\circ - \varepsilon - \eta$, the final expression is obtained [1], p113 :

$$\lambda = 90^\circ - \varepsilon - \arcsin \left(\cos (\varepsilon) \frac{R_E}{R_E + H} \right) \quad (5)$$

It is assumed that we want a continuous and complete coverage in what follows.

Two configuration are discussed here :

- Walker Star constellation or "Streets of coverage" constellation [3] (circular footprint), section 5.2
- Rectangular footprint constellation, section 5.2

- Rectangular footprint constellation with plane altitude separation, section 5.2

The inclination is the same for all planes and the altitude is also the same at first. Walker constellations are based on a simple design strategy for distributing the satellites in a constellation. There are two main variants of Walker constellations: Walker Delta constellations and Walker Star constellations. The two variants differ in the distribution of the ascending nodes between the planes of the constellation. For a Walker Delta constellation type, the ascending nodes of the planes are distributed over the full range of 360 degrees, while in the Star configuration, the ascending nodes are distributed over a 180 degree span.

The main issue with the Walker Delta constellation is that it is not an optimal solution to cover the whole Earth as each point on the equator is covered by an ascending node and a descending node, increasing by a factor two the number of plans required and therefore the total number of satellites. In order to have a less expensive solution, only the Walker Star constellations are considered.

The Walker Star constellation with circular footprint is a more academic one, however to be optimal and provide a full coverage each plane needs to be properly phased which can be tedious. The rectangular footprint constellation does not require any superposition of footprints and allow to have different orbital speed for each plane (independence of the planes), hence different altitudes for each planes. This choice also reduces the collision risk as planes close to each other will have different altitudes.

Walker Star constellation

For the Walker Star constellation, a circular footprint is considered with a radius of λ (seen as an angle from the Earth centre) (λ_{max} Figure 23).

A satellite spacing is defined as the distance between two consecutive satellite footprints on the ground track. A spacing coefficient s strictly between 0 and 2 is used to describe the superposition of the consecutive footprints. The number of satellite per plan is then given by :

$$N_{satPlanes} = \frac{2\pi}{s\lambda} \quad (6)$$

Note that at $s=0$ all circles are superposed and at $s=2$ there is no superposition at all, two subsequent circles share only one point. The superposition is used to ensure a continuous "street" of coverage to be sure to provide a continuous coverage, Figure 23. The size of the street is then :

$$\lambda_{street} = \arccos \left(\frac{\cos \lambda}{\cos \left(\frac{s\lambda}{2} \right)} \right) \quad (7)$$

It is the width of swath centred on the ground track for which there is continuous coverage, [1] p192.

The distance between two planes so that a continuous coverage is ensured is given by :

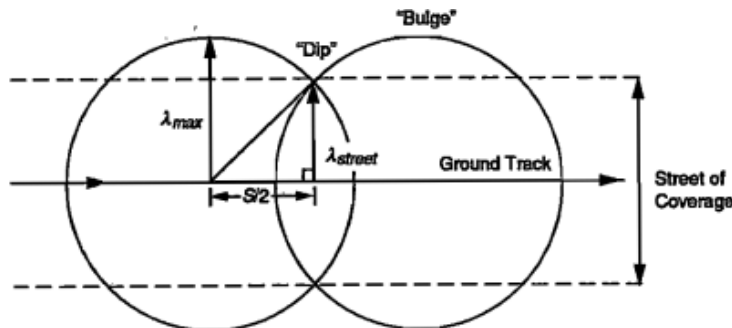


Fig. 7-10. The “Street of Coverage” is a Swath Centered on the Ground Track for which there is Continuous Coverage.

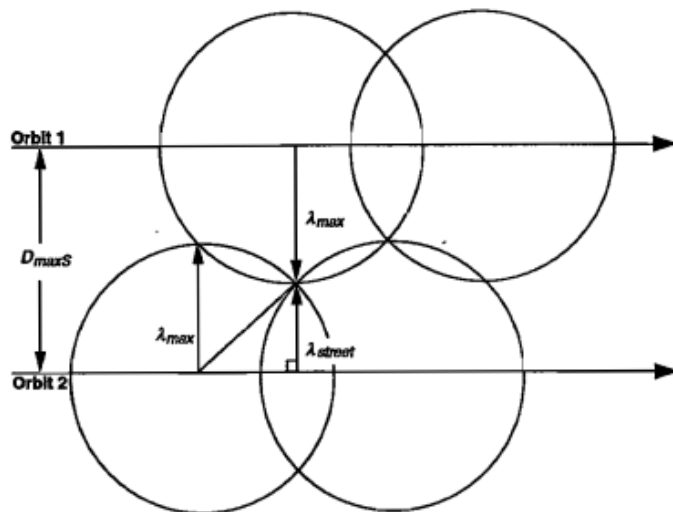


Fig. 7-11. Coverage in Adjacent Planes. If the planes are moving in the same direction, the overlap pattern can be designed to provide maximum spacing between adjacent planes.

Figure 23: Street of coverage and coverage in adjacent planes for the Walker Star constellation

$$D_{max} = \lambda + \lambda_{street} \quad (8)$$

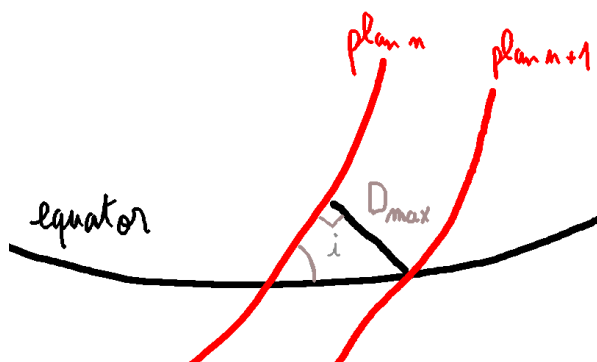


Figure 24: Ascending node of an orbit plane with respect to the next one

In order to cover the whole globe, there must be enough planes to cover half the equator with ascending part of the orbit (the descending one covers the other half by symmetry). Thanks to spherical trigonometry Figure 24, the separation distance between two planes at the equator is then given by :

$$D_{separation} = \arcsin \left(\frac{\sin D_{max}}{\sin i} \right) \quad (9)$$

Where i is the orbit inclination.

However one need to take into account that there need to be a smaller separation at the very last plane, Figure 25.

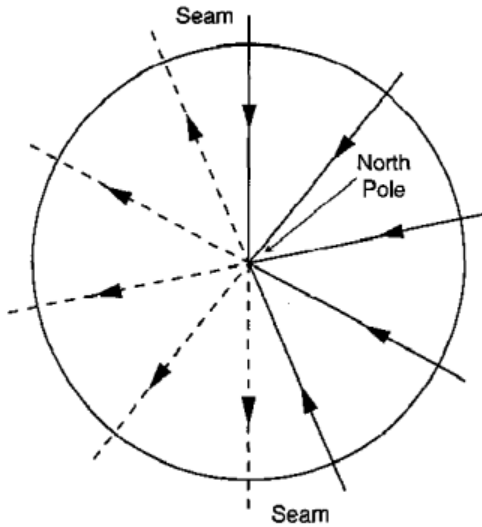


Figure 25: View seen from the North Pole. Northward portions of each orbit are shown in solid lines; southward portions are dashed

Indeed next to the last plane, there will be the descending node of the first plane : the optimisation with the dip and the bulge is not possible there. The following relation needs to be fulfilled [3] p687 :

$$(N_{planes} + 1)\lambda_{street_i} + (N_{planes} - 1)\lambda_i > \pi \quad (10)$$

Where

$$\lambda_{street_i} = \arcsin \left(\frac{\sin \lambda_{street}}{\sin i} \right)$$

and

$$\lambda_i = \arcsin \left(\frac{\sin \lambda}{\sin i} \right)$$

From the equation 10, one obtains :

$$N_{planes} > \frac{\pi - \lambda_{street_i} + \lambda_i}{D_{separation}} \quad (11)$$

However these formulas 10 and 11 are valid for polar orbits, with an inclination of 90° .

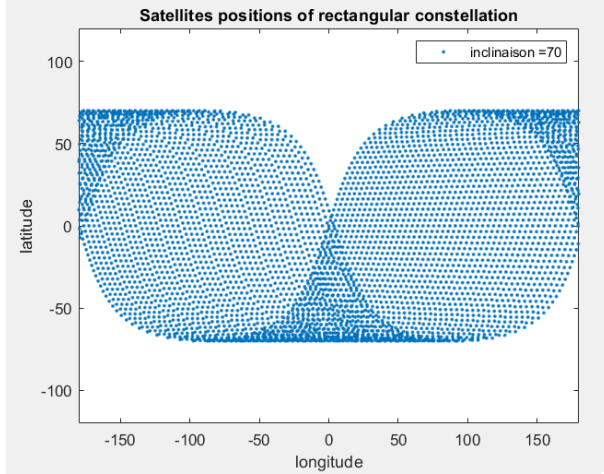


Figure 26: Position of the satellites with an inclination of 70 deg

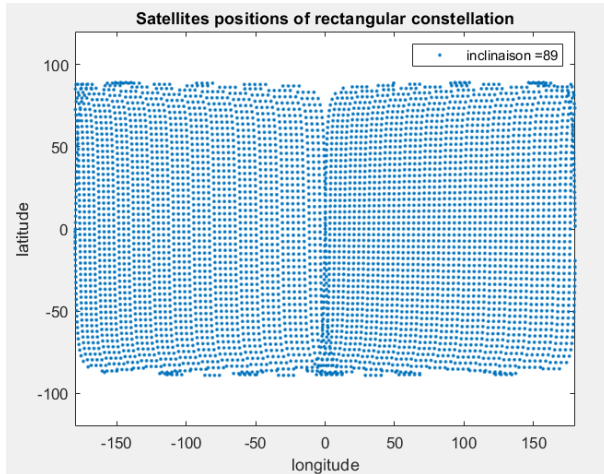


Figure 27: Position of the satellites with an inclination of 89 deg

Indeed if the inclination is smaller (or greater), a gap in the coverage appears at high north latitude above the ascending node of the first plane and at high south latitudes under the descending node of the first plane, Figure 26 and 27. In order to be sure to cover the globe up to $\pm 70^\circ$ of latitude, one can replace the angle to be covered at the equator, which was π in 10 and 11 by :

$$\text{AngleToCoverAtEquator}(i) = \pi + 2 \arcsin \left(\frac{\tan(70 * \pi / 180)}{\tan(i)} \right) \quad (12)$$

The equation comes from the intersection of two orbits, one at a RAAN of 0° and the other one at a RAAN of $\text{AngleToCoverAtEquator}(i)$ (which depends on inclination i) such that they intersect at 70° of latitude. One can notice that this $\text{AngleToCoverAtEquator}(i)$ is equal to π when $i=90^\circ$ which is consistent. Therefore the condition 11 is now :

$$N_{planes} > \frac{\text{AngleToCoverAtEquator}(i) - \lambda_{street_i} + \lambda_i}{D_{separation}} \quad (13)$$

Typical values are obtained with a Matlab script :

Walker Star Constellation (circular footprint) output

```

1
2 -----Walker Star Constellation (circular footprint)-----
3 Notice that the phasing between adjacent planes
4 should be sqrt(lambda^2-lambda_street^2) [rad]
5
6 Number of satellites : 7820
7 Number of planes : 46
8 Number of satellites per plane : 170
9 Inclination : 90 deg
10 Elevation min : 50 deg
11 Altitude : 300 km
12 Lambda (footprint radius from Earth) : 0.037126 rad ; 236.7879 km
13 Lambda Street : 0.032154 rad ; 205.0761 km

```

Notice that the order of magnitude of the first configuration proposed for the One Web constellation (648 satellites at 1200 km, inclination of 87.9° on 12 planes) is retrieved with a 50° minimum elevation angle :

Walker Star Constellation (circular footprint) output for One Web

```

1
2 -----Walker Star Constellation (circular footprint)-----
3 Notice that the phasing between adjacent planes
4 should be sqrt(lambda^2-lambda_street^2) [rad]
5
6 Number of satellites : 750
7 Number of planes : 15
8 Number of satellites per plane : 50
9 Inclination : 87.9 deg
10 Elevation min : 50 deg
11 Altitude : 1200 km
12 Lambda (footprint radius from Earth) : 0.12651 rad ; 806.854 km
13 Lambda Street : 0.10963 rad ; 699.223 km

```

Notice that the minimum elevation is a very sensitive parameter in the design process (here it is given and fixed).

Rectangular footprint constellation

Similar computations can be done with a rectangular footprint, with a width W (perpendicular to the ground track) and a length L (parallel to the ground track). Its maximum

dimension is 2λ , hence the diagonal of the footprint is equal to 2λ . The footprint is supposed to be parallel to the ground track, with its centre at the sub satellite point. If the number of satellites in a plan is chosen, the length L of the footprint is given by :

$$L = \frac{2\pi}{N_{satPlanes}} \quad (14)$$

With some spherical trigonometry, the width W is obtained :

$$W = \arccos \left(\frac{\cos 2\lambda}{\cos L} \right) \quad (15)$$

Two approaches are implemented in the simulation :

- the number of satellites per plane $N_{satPlanes}$ is fixed for all planes
- the ratio between length L and width W is fixed

In the last case, a search is performed for each altitude of plane in order to find the number of satellites per plane $N_{satPlanes}$ giving the closest ratio length L over width W targeted.

The separation of the planes at the equator is given by :

$$D_{separation} = \arcsin \left(\frac{\sin W}{\sin i} \right) \quad (16)$$

Where i is the orbit inclination. The number of planes is given by :

$$N_{planes} = \frac{\text{AngleToCoverAtEquator}(i)}{D_{separation}} \quad (17)$$

Typical values are obtained with a Matlab script :

Rectangular footprint Constellation output

```

1
2 —Rectangular footprint Constellation—
3
4 Satellites : 7200
5 Number of planes : 60
6 Number of satellites per plane : 120
7 Inclination : 90 deg
8 Elevation min : 50 deg
9 Altitude : 300 km
10 Mode : 1 (0:fixed NbSatPlan, 1:fixed Footprint Ratio)
11 Footprint Ratio : 0.99409
12 Footprint Width : 0.052671 rad ; 335.937 km
13 Footprint Length : 0.05236 rad ; 333.9513 km

```

Rectangular footprint constellation with plane altitude separation

The rectangular footprint constellation can be designed with a constant altitude separation ΔH between planes in order to lower the collision probability. This asset is crucial therefore the final design will be a plane altitude separation constellation. Each plane is populated with satellites in order to cover the whole plane. The next plane is then designed with a higher altitude, and the process is repeated until half of the equator is covered with ascending nodes, some planes are added if the orbits are not polar (see discussion about equation).

Rectangular footprint constellation with plane altitude separation output

```
1
2 -Rectangular footprint Constellation Plane Altitude Separation-
3
4 Satellites : 6287
5 Number of planes : 57
6 Inclination : 90 deg
7 Elevation min : 50 deg
8 Altitude from : 300 km to 356 km, equally spaced by 1 km
9 Mode : 1 (0:fixed NbSatPlan, 1:fixed Footprint Ratio)
10 Footprint Ratio : 0.99848
```

Walker Star and Rectangular footprint constellation

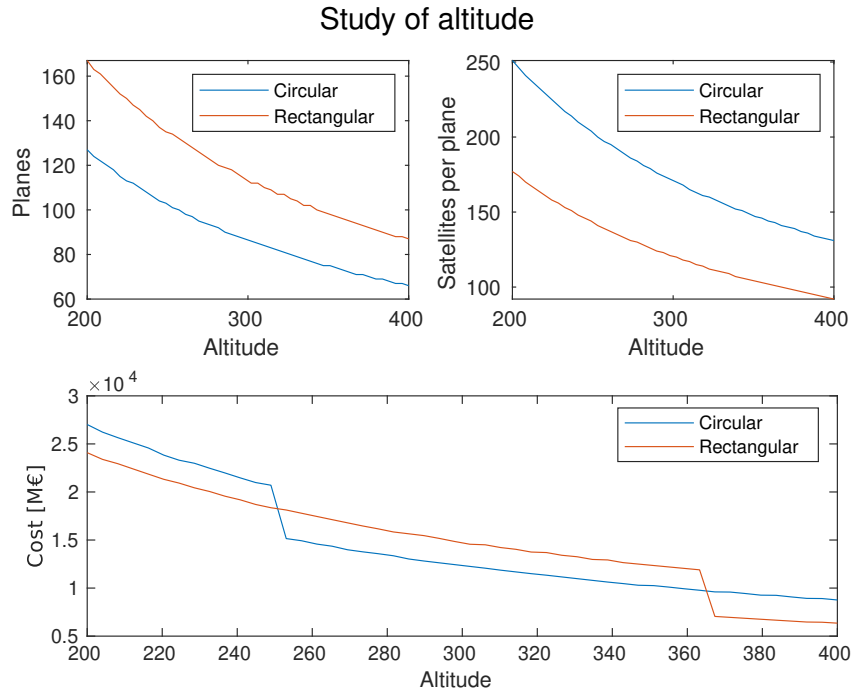


Figure 28: Number of planes, satellites per plane and cost function vs altitude

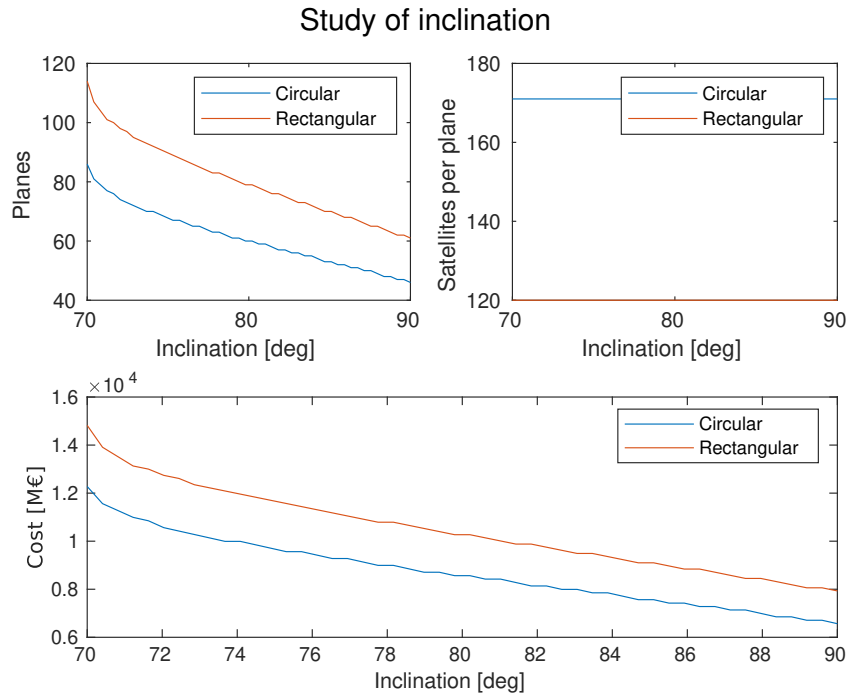


Figure 29: Number of planes, satellites per plane and cost function vs inclination

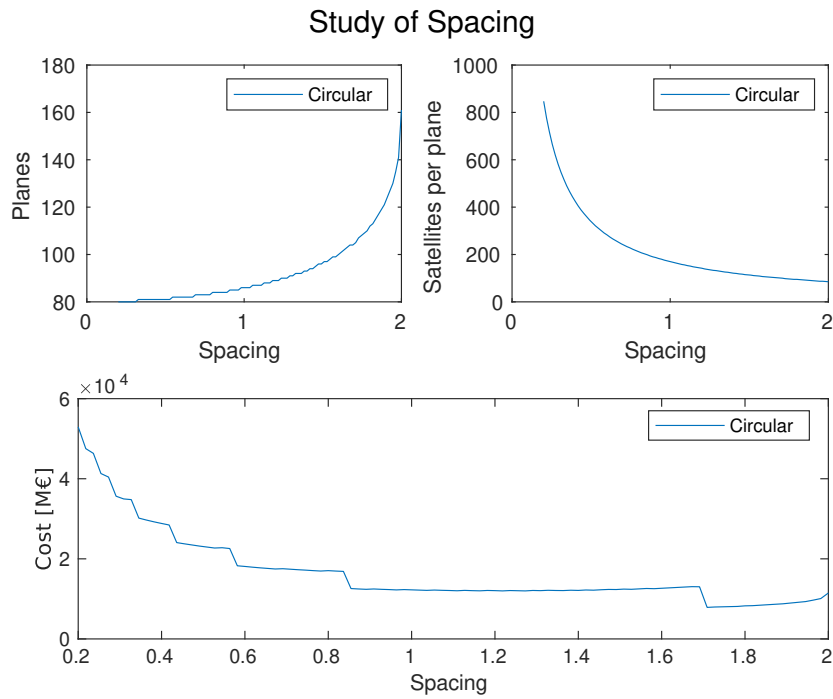


Figure 30: Number of planes, satellites per plane and cost function vs spacing

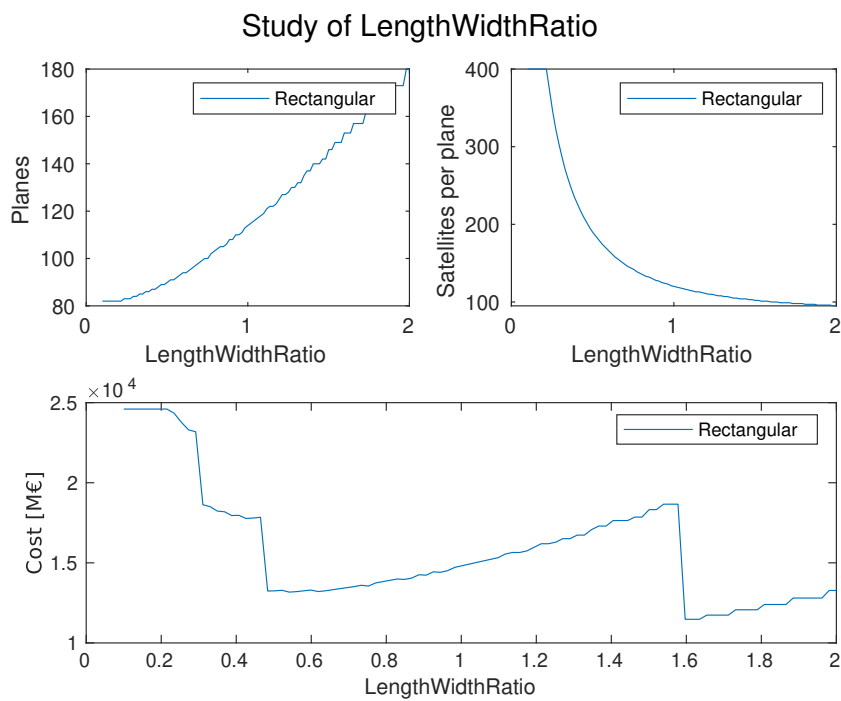


Figure 31: Number of planes, satellites per plane and cost function vs length over width ratio

The number of planes and satellites per planes decreases when the altitude increases therefore the best altitude to reduce the number of planes and satellites would be the highest, here 400 km, Figure 28. One can notice two stairs in the cost which are related to the "ceil" operation of the number of planes divided by 100. Indeed for the Walker Star circular footprint the stair occurs at 250 km, where the number of satellites per plane goes from more than 200 to less than 200. The same happens for the rectangular footprint at 370 km. Notice that just before the stair, it means that the whole plane can be launched at once except for a very few satellites : an alternative strategy might be possible to optimise the launches.

The inclination has no impact on the number of satellites per plane but is inversely proportional to the number of planes, Figure 29. Therefore the best inclination would be the largest one, 90° in order to be sure to cover the globe perfectly.

The spacing parameter in the Walker Star constellation with a circular footprint shows a minimum around 1.7, which is not easily derived by hand, Figure 30. A large spacing means that the street of coverage is reduced, hence increasing the number of planes and decreasing the number of satellites per planes required as they are more spaced along one orbital plane. A spacing of 2 is the limit in order to ensure a full coverage.

The ratio between the length and width Figure 31 shows plateaus where the optimal value is around 0.5, even if the value 1.65 gives a very similar cost. The larger the width is, the smaller the number of planes get and the larger the number of satellites per plane get.

Rectangular footprint constellation with plan altitude separation

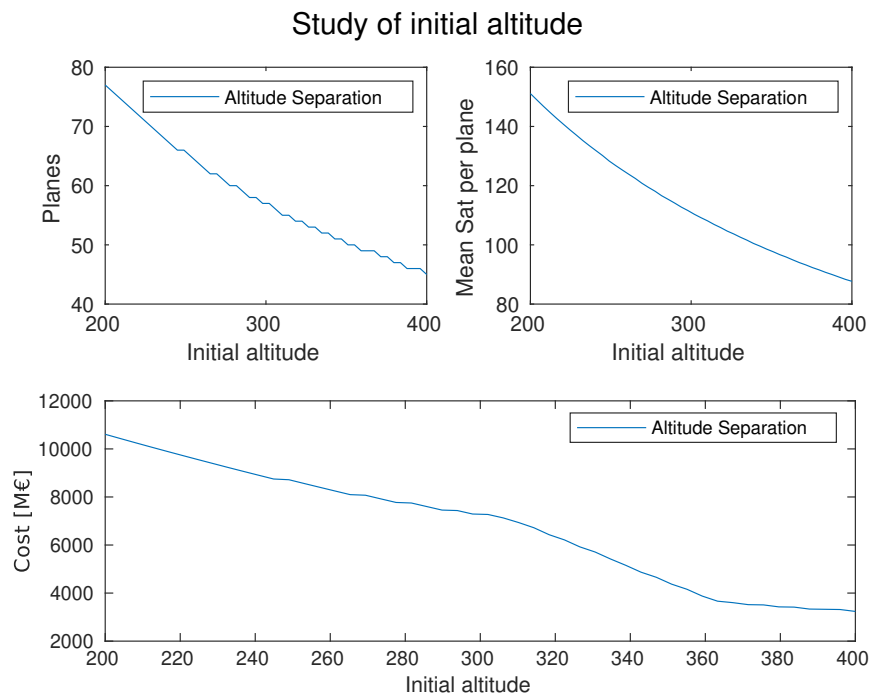


Figure 32: Number of planes, satellites per plane and cost function vs initial altitude

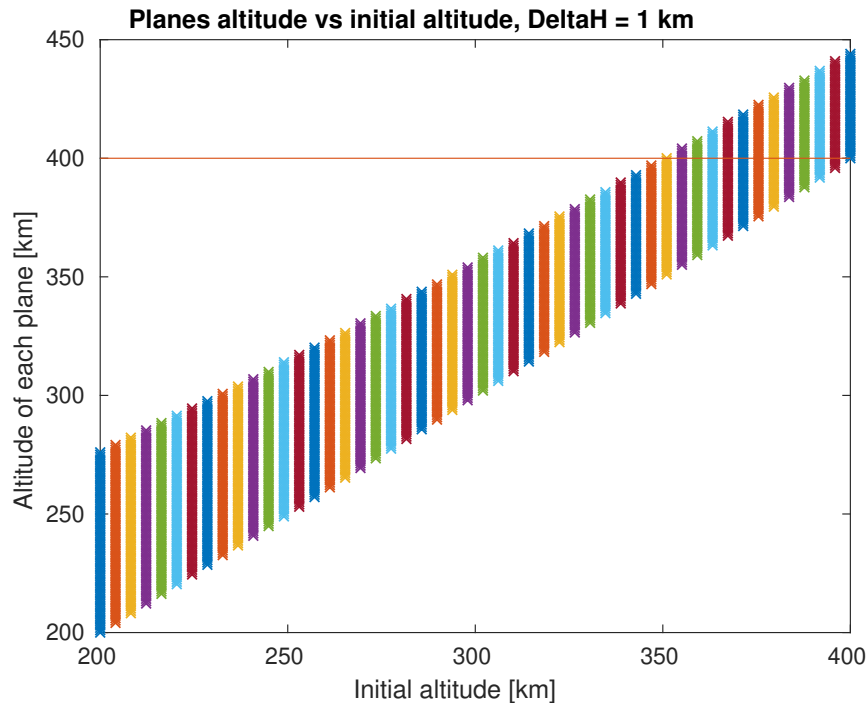


Figure 33: Altitude of each plane vs initial altitude

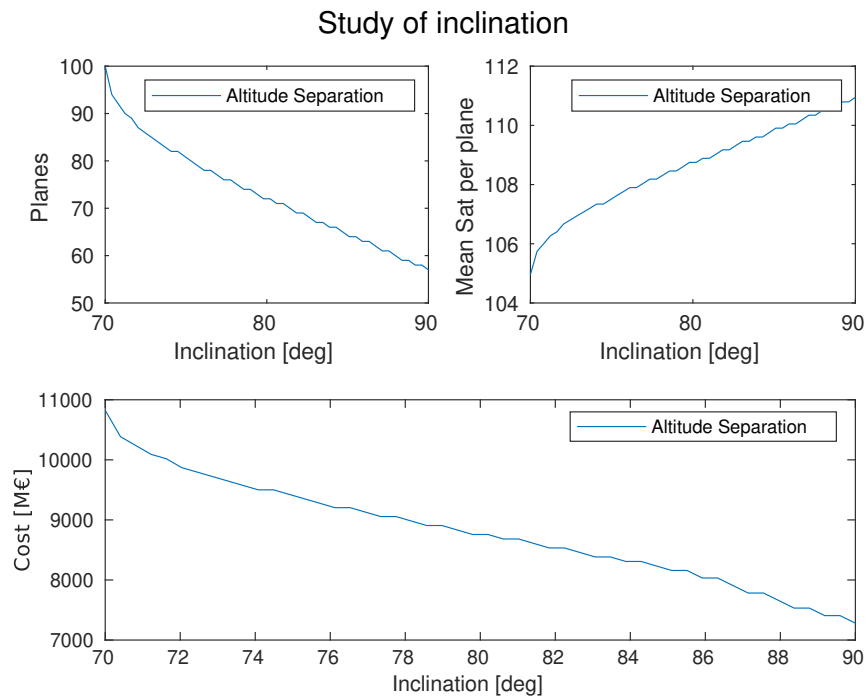


Figure 34: Number of planes, satellites per plane and cost function vs inclination

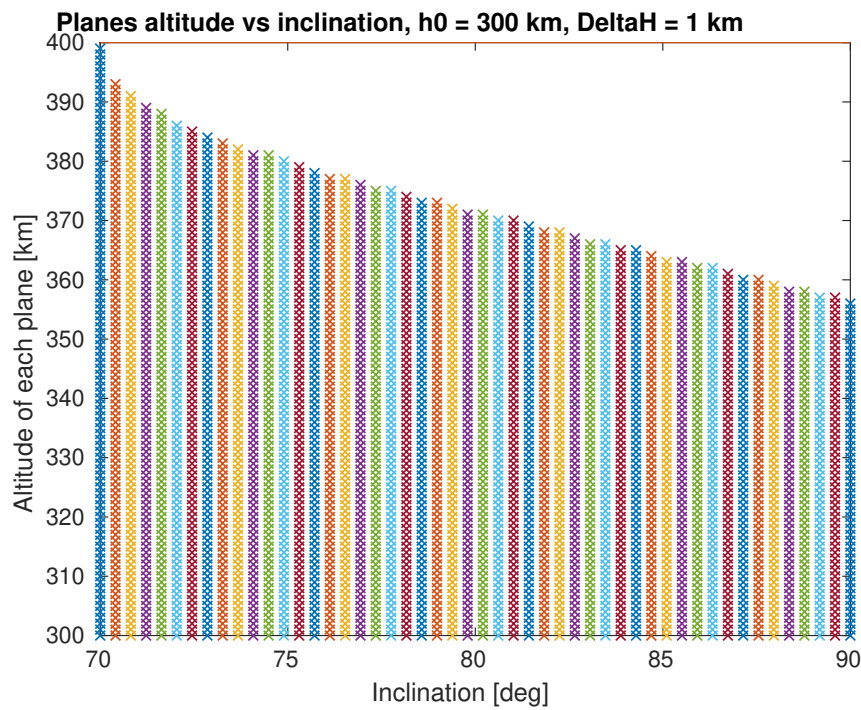


Figure 35: Altitude of each plane vs inclination

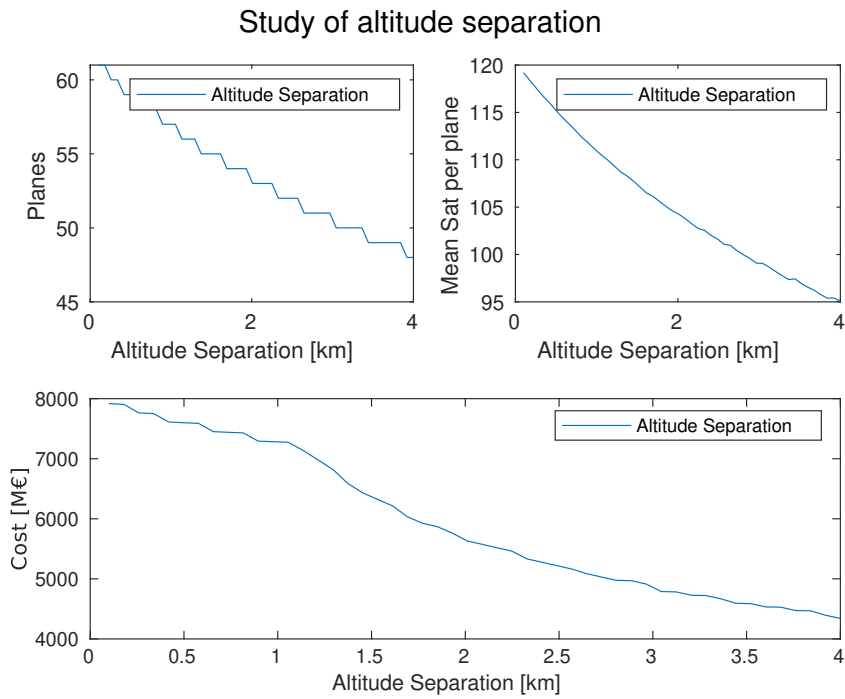


Figure 36: Number of planes, satellites per plane and cost function vs plane altitude separation

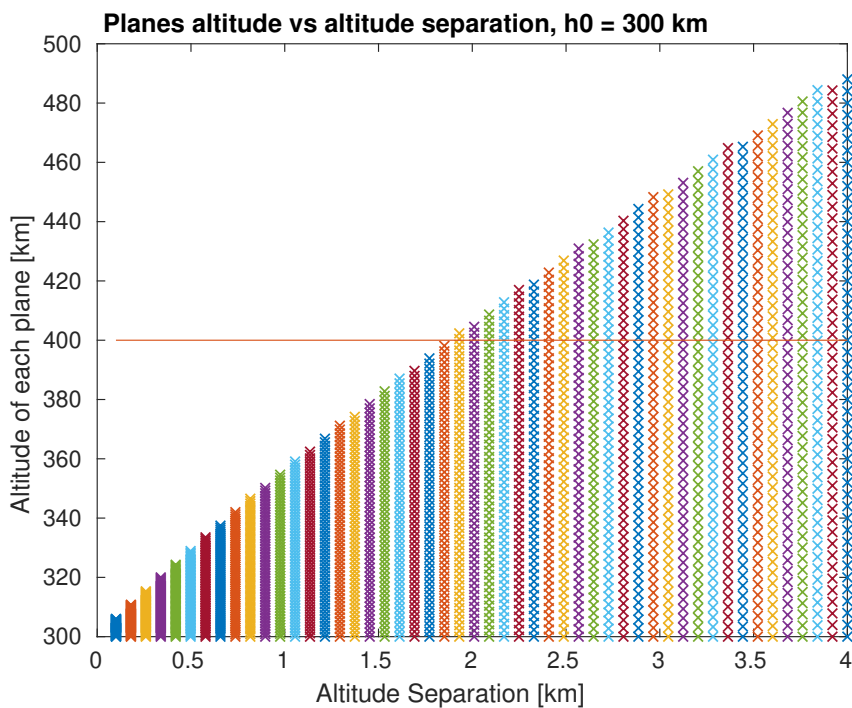


Figure 37: Altitude of each plane vs plane altitude separation

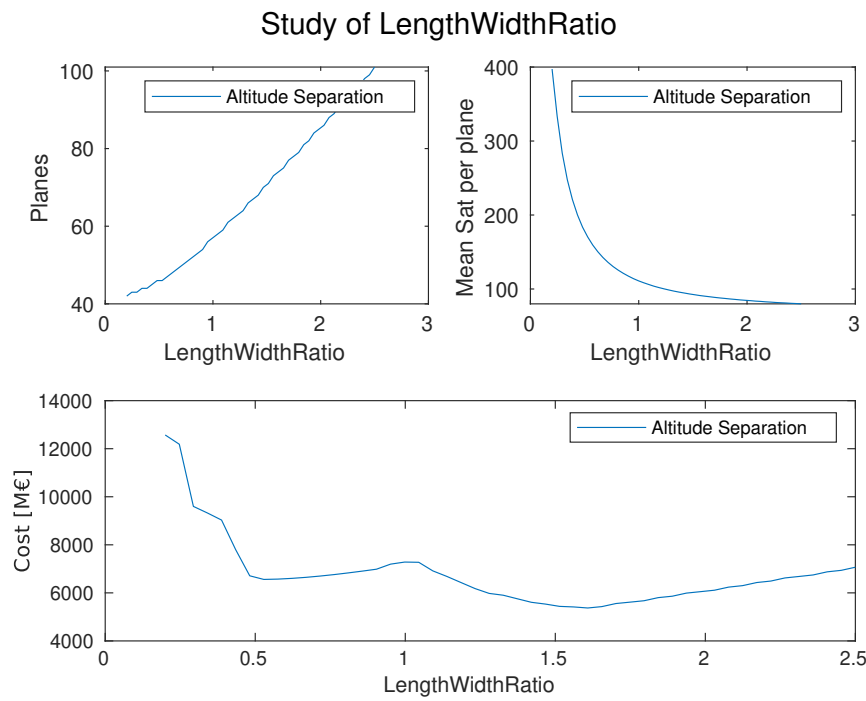


Figure 38: Number of planes, satellites per plane and cost function vs length over width ratio

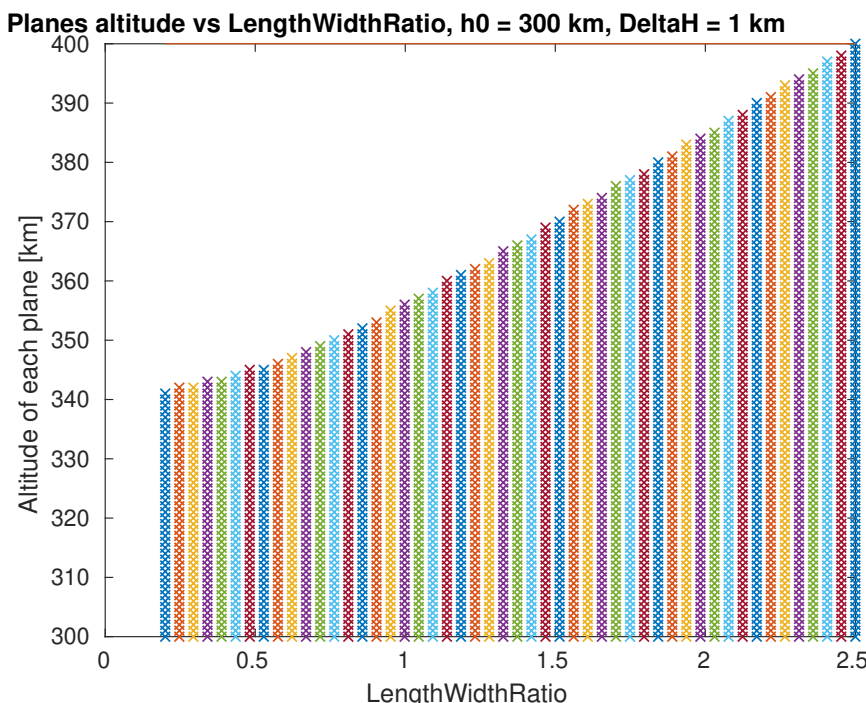


Figure 39: Altitude of each plane vs length over width ratio

The initial altitude Figure 32 shows that the best for the cost function is to select a high initial altitude as the previous analysis showed. However there is an upper limit to the initial altitude as the last plane has to be lower than 400 km, Figure 33, about 350 km for a Δ_H of 1 km. This graph shows that less planes are required when the initial altitude is larger.

The study of inclination Figure 34 and 35 shows that in order to optimise the cost the inclination should be the closest to 90° . Indeed if the inclination is not polar, additional planes need to be considered to cover the whole zone of $\pm 70^\circ$, hence it requires more satellites leading to a greater cost. Therefore a (quasi) polar orbit should be selected.

The study of altitude separation between planes shows that a larger altitude separation improves the number of planes and of satellites per plane, Figure 36 and 37. It is directly linked to the fact that higher altitudes are used and therefore the field of view increases, reducing the number of satellites to cover the same area. Notice however that there is an upper limit to this altitude separation fixed by 400 km the altitude of the ISS, corresponding here to an altitude separation of 2 km for a starting altitude at 300 km.

The study of the ratio between length and width shows a minimum at 1.6 which is not trivial to obtain analytically, Figure 38 and 39. This parameter depends on the altitude parameters and the values in the cost function.

ISS constraint

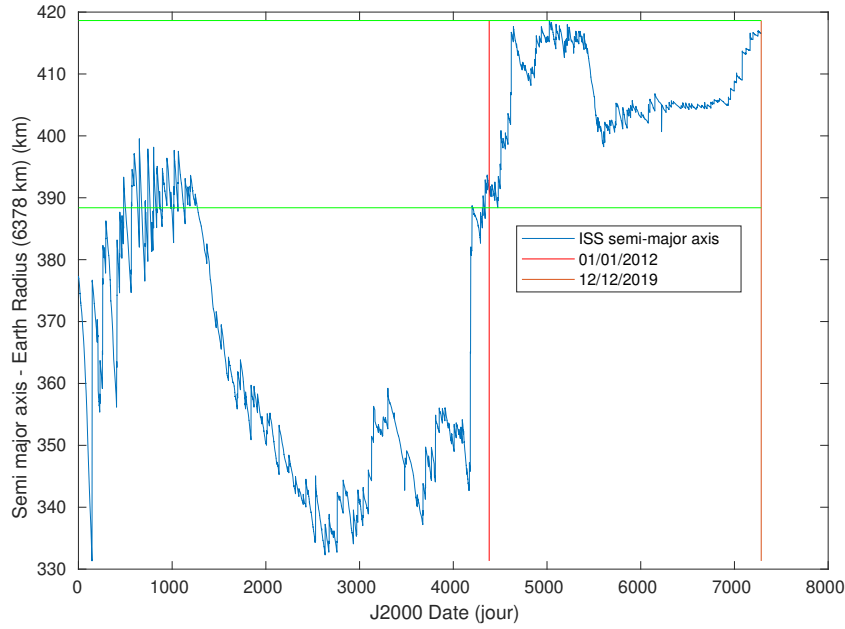


Figure 40: Semi major axis minus the Earth radius of the ISS (km)

It is clear that for safety reasons, the orbits of the constellation should not cross the ISS. The TLE (Two Line Elements) of the ISS are recovered from www.space-track.org and the semi-major axis minus the Earth radius (6378 km) is displayed versus time Figure 40. Since the 1st January 2012, the lowest semi-major axis is 6766 km, that is to say 388 km. This altitude will be the upper limit for the altitudes of the constellation.

Analysis of the cost

The rectangular footprint constellation with plane altitude separation is selected for its properties reducing collision and removing the need of in-phase planes. The inclination selected is polar, 90° and the altitude separation between two planes is fixed at 1 km (loss of altitude after 10 orbits at 300 km).

The figures 42 to 53 describe the cost with respect to the initial altitude and the length to width ratio or the number of Satellites per plane show different features :

- the cost is smaller for higher altitudes
- some plateaus can be identified and the overall look of the cost function is in stairs due to the discrete values of the problem (number of satellites, number of planes)

Some pixels are blank : either it is because the ISS constraint is not fulfilled (all the satellites should be at altitudes lower than 400 km) or the problem is unfeasible (not enough satellites per plane to cover the whole plane). The simple cost analysis shows that the best is always to go the highest possible to minimise the cost, Figure 44 to 46 and Figure 50 to 51.

Without the ISS constraint, there is an optimum with the advanced cost function that appears Figure 48 and 52. However with the ISS constraint the optimum are at the border of the admissible set, Figure 49 and 53. Notice that for the simple cost the optimum is already at the border of the admissible set, at the highest initial altitude possible (here the maximal initial altitude tested is 400 km).

The optimal solutions are reported table 15 and 14. It is not an interesting result as there is no optimum for the constellation features and the it appears that the best is to go for the highest altitudes possible to minimise the cost.

| | Satellites per plane | Length/Width ratio | h_0 (km) | Cost |
|---|----------------------|--------------------|------------|--------|
| Satellites per plane | 148 | - | 371.86 | 2651.4 |
| Satellites per plane (ISS constraint) | 160 | - | 347.7 | 2757.9 |
| Satellites per plane $\Delta_h = 0.5$ (ISS constraint) | 142 | - | 367.34 | 2672.7 |
| Length/Width ratio | - | 0.5 | 372.24 | 2654.6 |
| Length/Width ratio (ISS constraint) | - | 0.54 | 347 | 2764.2 |

Table 14: Optimal solution obtained with the advanced cost function

A sensibility study was performed on the cost function with respect to the parameters of the launch cost, the cost function of one satellite with respect to the altitude, the launch vehicle capacity with respect to the altitude and the mass of one satellite with respect to the altitude. Homothetic variations were applied to the last three functions.

| | Satellites per plane | Length/Width ratio | h_0 (km) | Cost |
|---|----------------------|--------------------|------------|--------|
| Satellites per plane | 98 | - | 399.49 | 3054.5 |
| Satellites per plane (ISS constraint) | 100 | - | 334.7 | 3900 |
| Satellites per plane $\Delta_h = 0.5$ (ISS constraint) | 99 | - | 362.4 | 3662.8 |
| Length/Width ratio | - | 0.85 | 400 | 3102 |
| Length/Width ratio (ISS constraint) | - | 1.2 | 330.6 | 4179.5 |

Table 15: Optimal solution obtained with the simple cost function

It appears that with the ISS constraint the optimum stays the same for a launch cost between 30 M€ to 70 M€ and homothetic variations between -50% to +50%. The optimum stays the same when there are variations of the launch cost.

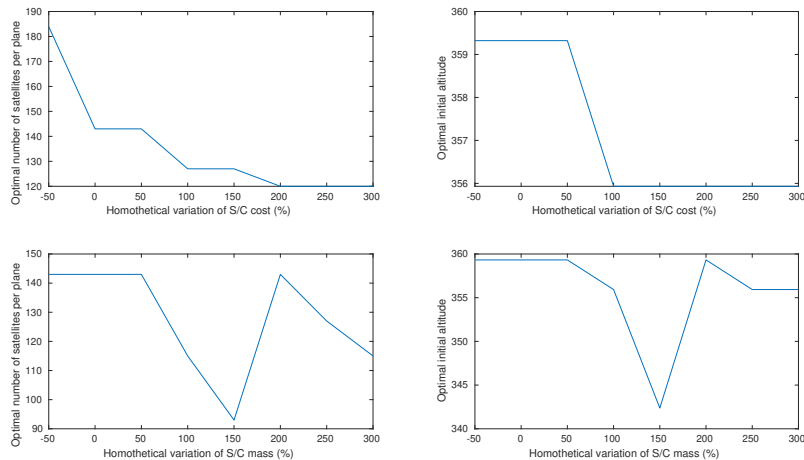


Figure 41: Analysis of the sensitivity of the optimal solution, for the cost of a satellite (top) and its mass (bottom)

However this optimum changes if the ISS constraint is removed : the initial altitude decreases with the launch cost, when the cost of one satellite decreases, the initial altitude increases and when the mass of one satellite increases, the initial altitude decreases. These results are shown Figure 41, however more points should be obtained to better understand the variations of the optimal parameters with respect to the sensibilities applied.

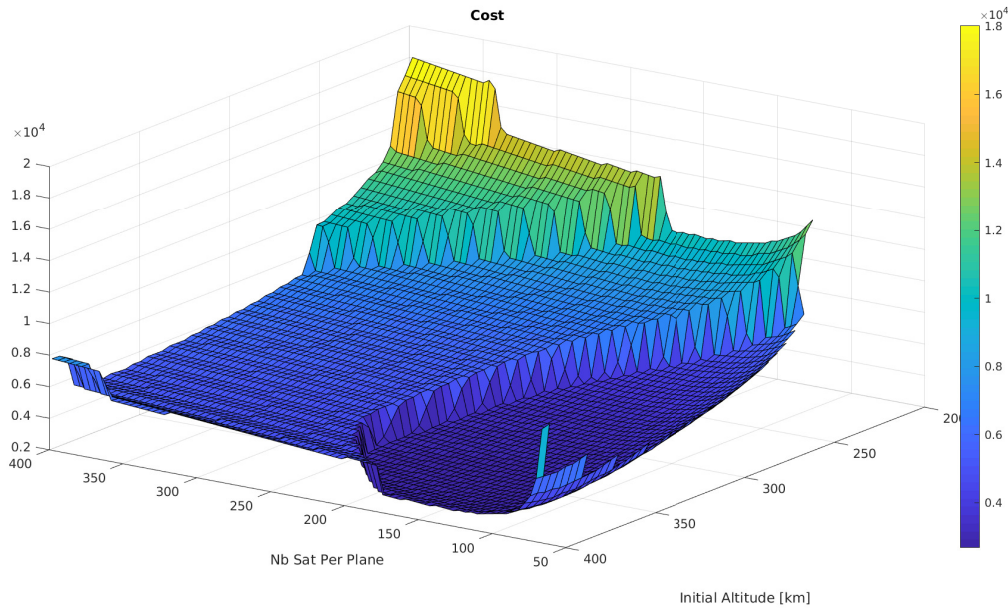


Figure 42: Advanced cost function vs Number of satellites per plane and Initial Altitude (3D view)

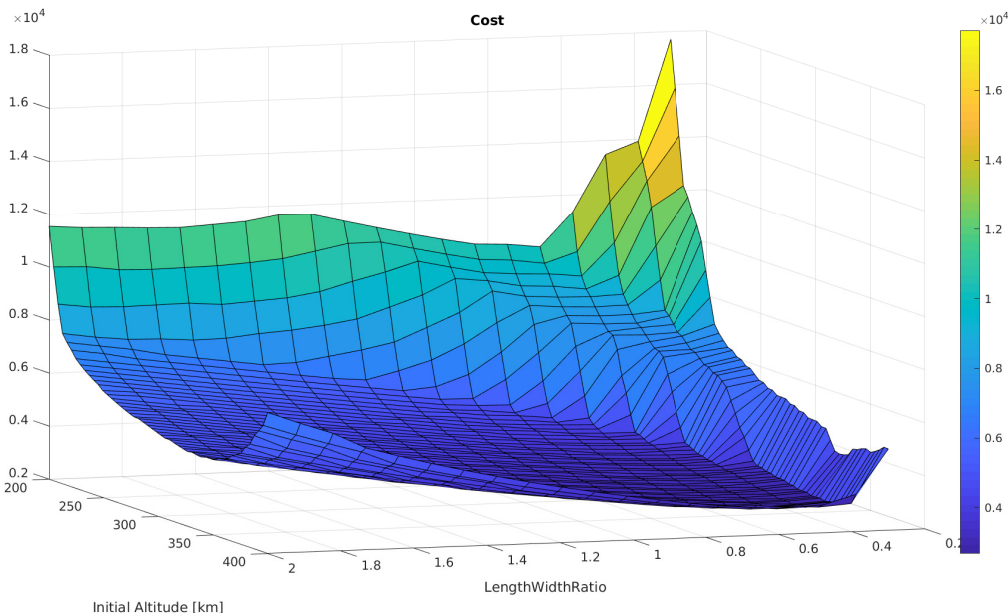


Figure 43: Advanced cost function vs Length/Width ratio and Initial Altitude (3D view)

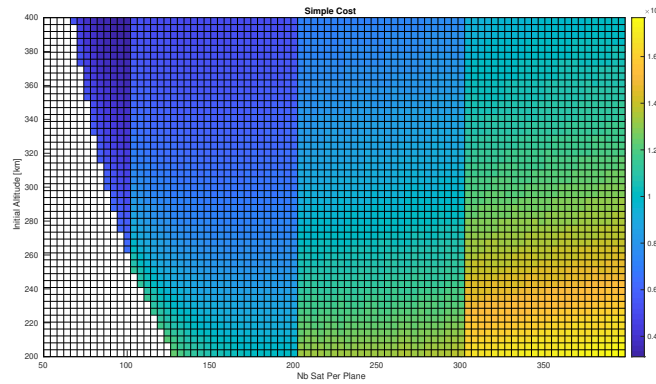


Figure 44: Simple cost function vs Number of satellites per plane and Initial Altitude

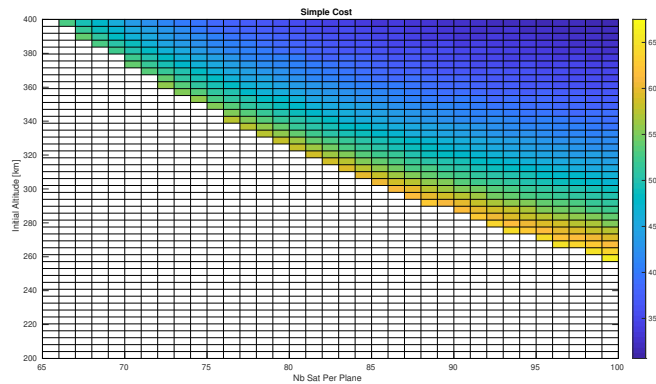


Figure 45: Simple cost function vs Number of satellites per plane and Initial Altitude (Zoom)

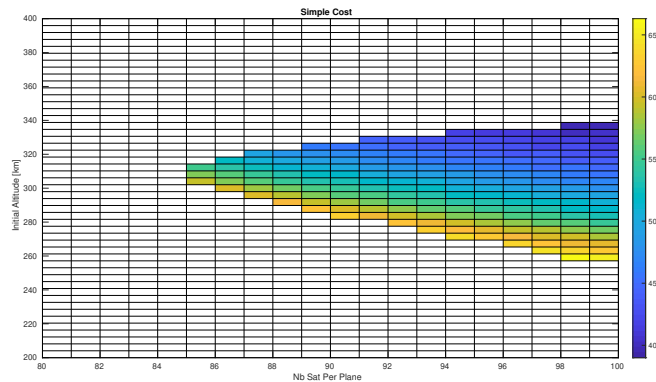


Figure 46: Simple cost function vs Number of satellites per plane and Initial Altitude with the ISS constraint (Zoom)

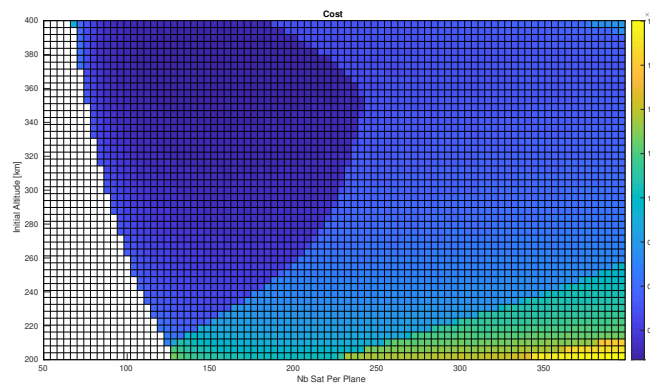


Figure 47: Advanced cost function vs Number of satellites per plane and Initial Altitude

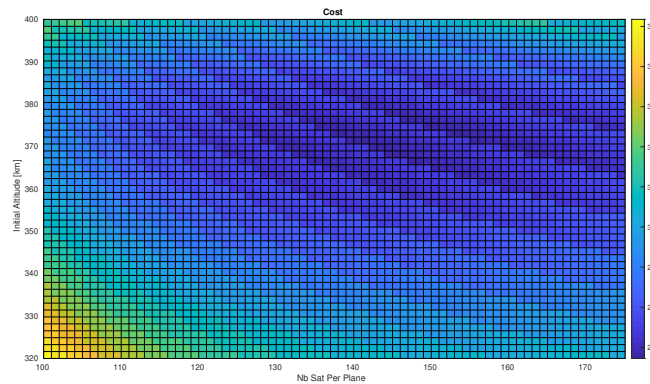


Figure 48: Advanced cost function vs Number of satellites per plane and Initial Altitude (Zoom)

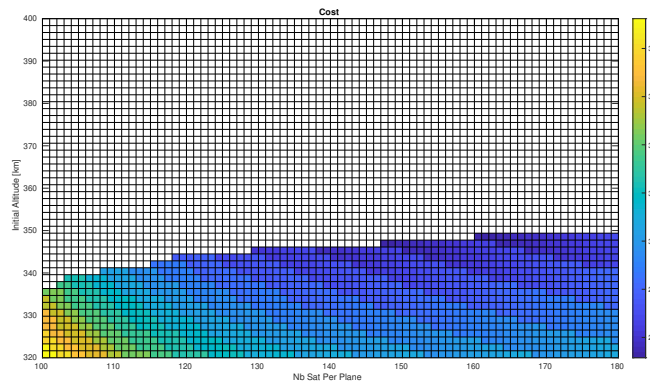


Figure 49: Advanced cost function vs Number of satellites per plane and Initial Altitude with the ISS constraint (Zoom)

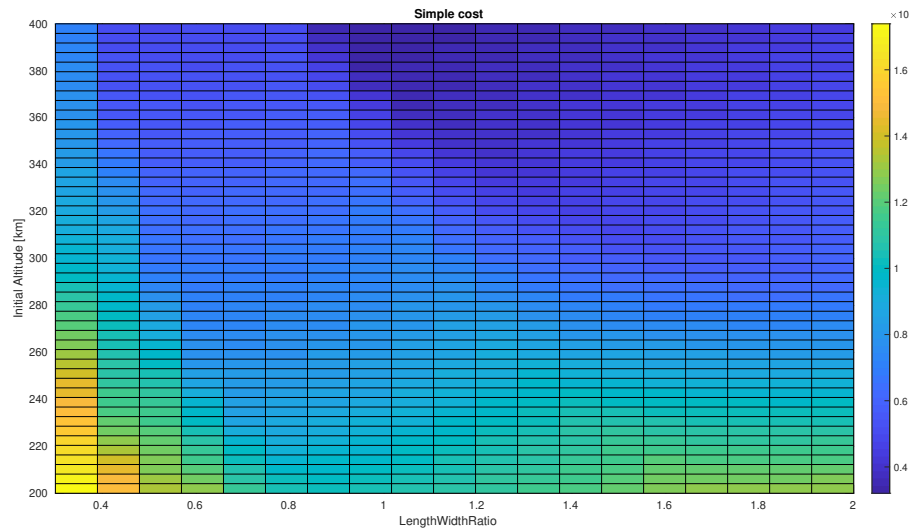


Figure 50: Simple cost function vs Length/Width ratio and Initial Altitude

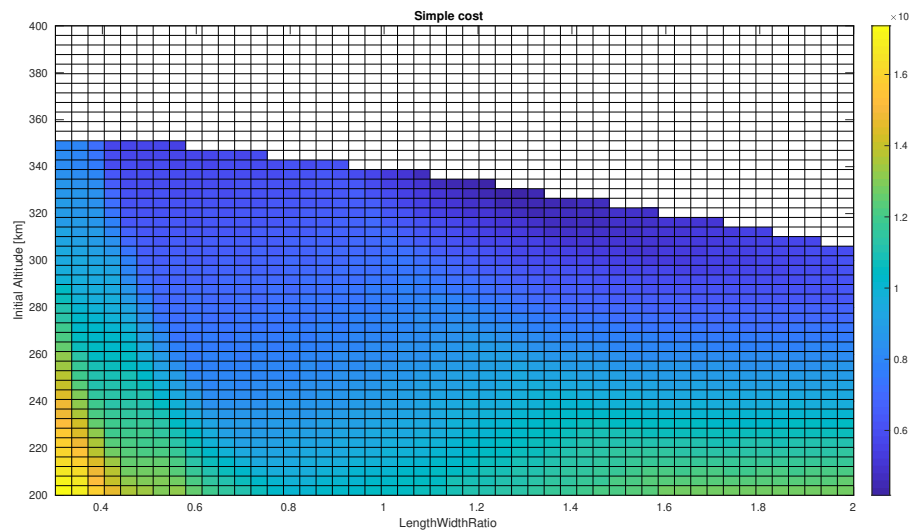


Figure 51: Simple cost function vs Length/Width ratio and Initial Altitude with the ISS constraint

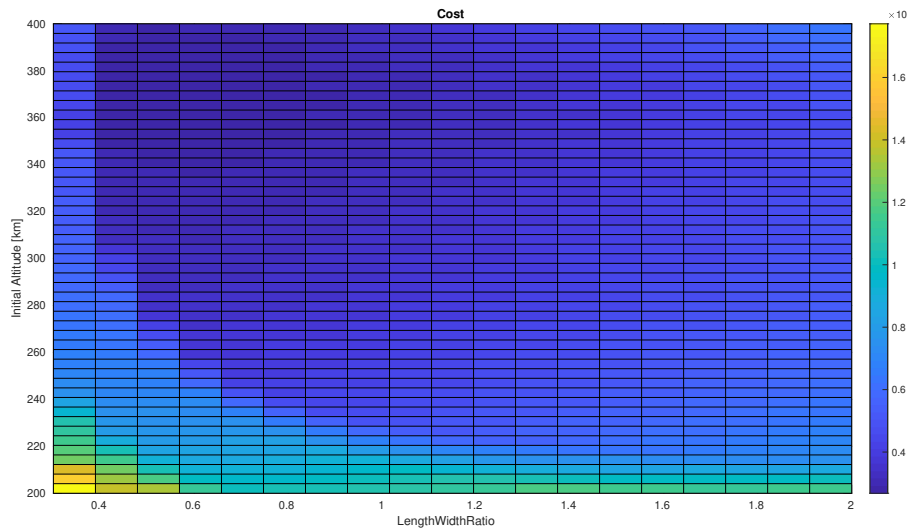


Figure 52: Advanced cost function vs Length/Width ratio and Initial Altitude

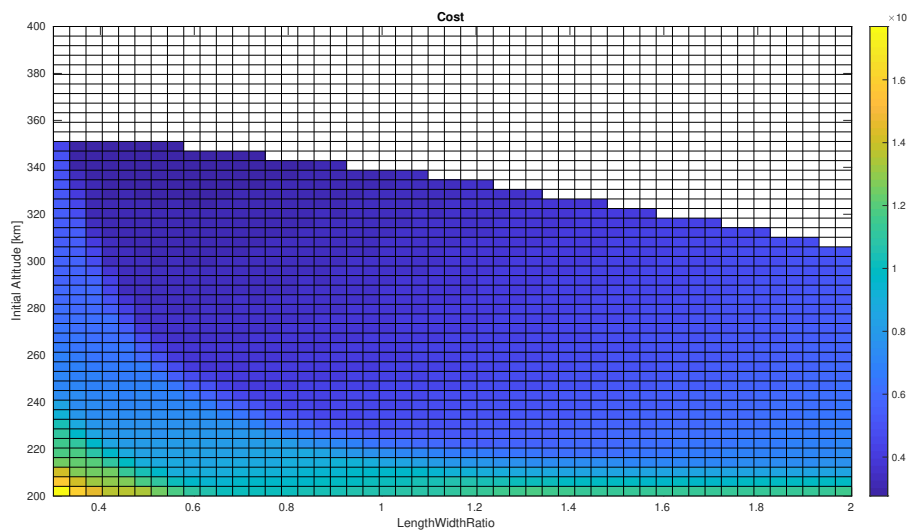


Figure 53: Advanced cost function vs Length/Width ratio and Initial Altitude with the ISS constraint

5.3 Optimal number of Gateways

The optimal number of gateways depends on the initial spacing chosen and the altitude of satellites, if we use a naive solving method we can see how the number of gateways evolves with the initial altitude of the constellation :

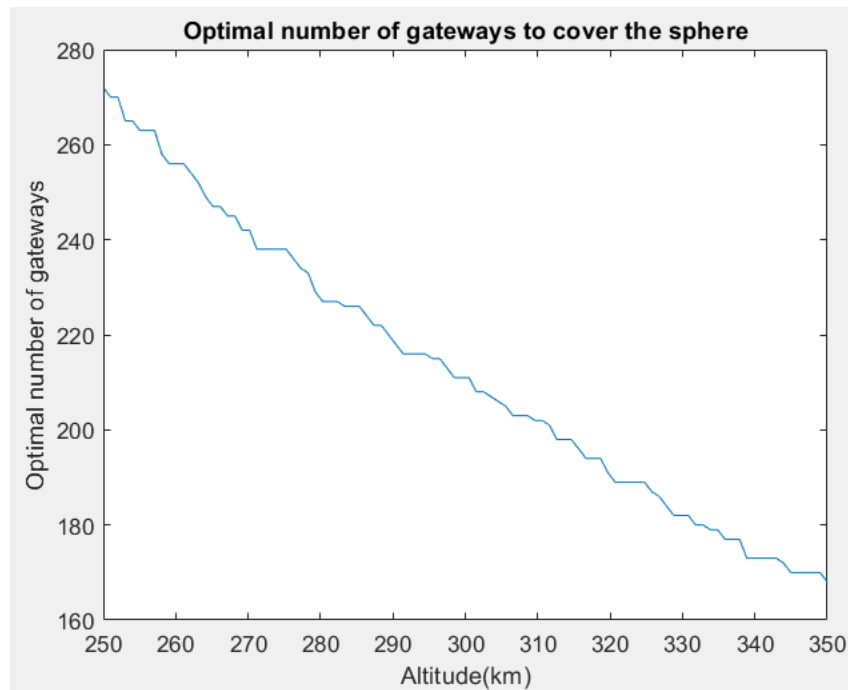


Figure 54: Optimal gateways number with respect to the altitude

5.4 Reliability and spare management

Oversizing the payload / Hot spares

This strategy involves to oversize the payload or equivalently to put more active satellites per plane than needed such that the failure of a few non consecutive satellites still covers the ground correctly to have a quality of service of 99.5%. Indeed, the satellites are designed such that the area covered on the ground by the mission is the maximum, directly related to the altitude and maximum elevation (50°) for the user, therefore it is not possible to increase the area covered by the payload by only oversizing the payload.

Here the time to replace a failed satellite is the time needed to rephase the plane. Each plane is separated by 1 km, therefore the orbit used for the phasing is constrained. In order to provide the maximum phase drift, the simplest scenario is to perform a first Hohmann transfer to put the satellite on a circular phasing orbit above or under its nominal orbit and then performing a second Hohmann transfer to come back to the nominal orbit at the proper place. The phasing orbit altitude need to be ± 1 km with respect to the nominal altitude to avoid a collision with the plane above or under.

From N satellites on one plane, if a satellite fails at an angle θ_{fail} , all the other satellites need to be rephased to be evenly spread on the plane. Two different cases arises, if N is even or odd, table 16. The new angle origin is the satellite that does not need to move during the phasing maneuver : it will be the new reference for the relative phase. The optimal choice is to set the new reference at the satellite opposite to the failed satellite to reduce the phase gap. The maximum phase gap to catch up is $\frac{180}{N}$ for all cases. This phase sets the time for the whole phasing maneuver. If N is even, $\frac{N}{2} - 1$ satellites have a phase lag (phasing orbit will be lower), $\frac{N}{2} - 1$ satellites have a phase lead (phasing orbit will be higher) and one satellite does not need to move. If N is odd, the configuration is not symmetrical anymore and to be optimal (fastest solution), the new angle origin need to be chosen to let $\frac{N-1}{2}$ satellites in phase lag, $\frac{N-1}{2} - 1$ satellites in phase lead and one satellite that stays at the same position. Examples of odd and even configurations are displayed Figure 56.

| | New angle origin (deg) | Maximum phase gap (deg) |
|-------------|---|--|
| N is odd | $\theta_{fail} + 180 \pm \frac{180}{N}$ | $\frac{180}{N}$ |
| N is even | $\theta_{fail} + 180$ | $\frac{360}{N} - (180 - (\frac{N}{2} - 1))\frac{360}{N-1} = \frac{180(N-2)}{N(N-1)}$ |

Table 16: Phases for the different cases with N the number of satellites per plane

Let us consider the case where the number of satellites per plane N is equal to 160 giving a maximum phase difference of 1.125° . The longest time to do the phasing is obtained at the highest altitude (around 387 km for the constellation designed here). For the following computation, the orbit nominal altitude is 387 km. The duration of the maneuver for different altitude of the phasing orbit are displayed Figure 57 and the cost associated to the two Hohmann maneuvers Figure 58. Notice that the computation of the worst case is given here for the phase lag case, i.e. the satellite needs to speed up to catch up with its new nominal position. In the phase lead case, the phasing orbit is above the nominal orbit and the total time is slightly longer (40 s longer).

With a respectable margin, a phasing orbit at half a kilometer under or above the nominal orbit gives a phasing time from 160 to 159 satellites of 42 h 34 min. For more active satellites in the plane, the phasing time for one satellite failure is shorter, about 34 h for 200 satellites in the plane, Figure 55.

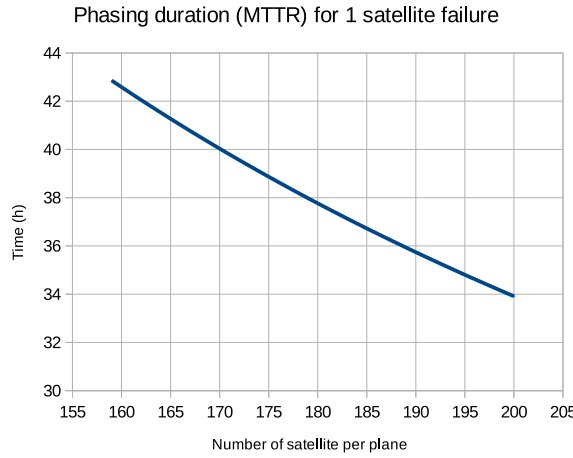


Figure 55: Phasing maneuver duration for a plane at 387 km (worst case for the constellation) for the failure of one satellite with respect to the number of active satellite in the plane before the failure.

In plane idle spares

There are two different strategies after one failure :

- only the idle satellite closest to the failed satellite goes into a phasing maneuver to replace the failed satellite in the plane
- several satellites do a phasing maneuver to let the idle satellite insert as a nominal satellite of the plane

The first strategy is clearly the longest one, and the phase to catch up with is $\frac{180}{\tilde{N}}$ degrees where \tilde{N} is the number of idle satellites evenly distributed within the nominal plane. So the best way to reduce the maneuver duration in this case is to increase the number of idle satellites per plane \tilde{N} , Figure 59.

The second strategy involves more satellites, but the time to replace one satellite cannot be reduced and will nearly always be $\frac{360}{N_0}$ where N_0 is the number of nominal satellites in the plane, that is to say for a 387 km nominal altitude and a phasing orbit at \pm half a kilometer, time to replace one satellite = 85 h 55 min. Indeed all the nominal satellites between the failed satellite and the closest idle satellite will maneuver to shift of one position so that the failed satellite is replaced and the idle satellite can insert itself correctly. Notice that the very best case would be that the failed satellite is the closest to the idle one, in this case the time to replace one satellite would be reduced and only the idle satellite is maneuvered. Here the number of idle satellites will have a

role in the number of satellites that need to be maneuvered, meaning using more fuel and possibly disturbing the service during the maneuver. The number of nominal satellites to be maneuvered can be estimated by $\frac{N_0}{2N}$, table 17. It requires 81 spare satellites for the first idle spare strategy to be as fast as the second spare strategy.

| | | | | | | | | | | | |
|--------------------------------------|----|----|----|----|----|----|----|----|----|----|----|
| Idle spare satellite (\tilde{N}) | 8 | 12 | 16 | 20 | 24 | 28 | 32 | 36 | 40 | 44 | 48 |
| Nominal satellites to be maneuvered | 10 | 7 | 5 | 4 | 4 | 3 | 3 | 3 | 2 | 2 | 2 |

Table 17: Number of nominal satellites to be maneuvered for the second idle spare strategy

Above planes of spares

Above planes of spares : one or several planes are above the ISS with an inclination smaller than 90° in order to use the RAAN drift to catch up with the plane where the failed satellite is.

The strategy to replace a failed satellite can be detailed :

- The above plane need to have the correct RAAN in order for the new satellite to be in the correct plane
- Do a maneuver to obtain the correct inclination to set the RAAN
- Use this orbit above the ISS with the correct RAAN as a phasing orbit
- Do a Hohmann transfer to put the new satellite at the right position

The drift of the RAAN is described by :

$$\dot{\Omega} = -\frac{3}{2} \left(\frac{R_{eq}}{a} \right)^2 \frac{n J_2 \cos(i)}{(1-e^2)^2} = -\frac{3}{2} \left[\frac{\sqrt{\mu} J_2 R_{eq}^2}{(1-e^2)^2 a^{7/2}} \right] \cos(i)$$

With n the mean motion of the satellite, R_{eq} the Earth radius, i the inclination of the orbit, e its eccentricity and a the semi-major axis of the orbit. Once the correct RAAN is obtained, a maneuver is performed at the node to put the satellite on a 90° orbit, setting the RAAN of the correct plane. Then the satellite waits on its orbit before performing a Hohmann transfer to be positioned exactly at the correct spot in the plane that need to be replenished.

The altitude of the spare plane is chosen to be 450 km (an orbit too high would waste maneuver time and too low would be too close to the ISS). The duration of the phasing maneuver with respect to the initial phase difference is described Figure 60, going from 70 hours to no need of phasing. Four planes evenly spread are chosen instead of one in order to reduce the waiting time due to the RAAN : therefore the maximum $\Delta\Omega$ to catch up is $\frac{\pi}{8}$. The eccentricity of the spare plane is chosen to be 0, however such variable can be used to increase the RAAN drift, and such possibility could be explored. The Figure 61 shows that the time of maneuver grows exponentially with the inclination, therefore

the lowest inclination possible should be selected. However as the inclination is smaller, the cost of the maneuver increases a lot. Notice also that the number of above planes might also be increased to reduce the RAAN angle to catch up, depending on the number of spares to be launched.

Discussion about the eccentricity

The formula for the RAAN drift suggest that some gain can be obtain by using the eccentricity of the orbit. However there is a limit here as the perigee of the spare orbit need to be higher than the ISS, that is to say 400 km at least (margins should be used). Therefore for one semi-major axis a given, there is an upper limit for the eccentricity : $e < 1 - \frac{400+6378}{a}$. One idea to maximize $|\dot{\Omega}|$ is to increase the upper limit of e by increasing a . However, with $e = 1 - \frac{400+6378}{a}$, $|\dot{\Omega}|$ decreases when a increases. Then the only option left is to have the lowest possible perigee and the same semi-major axis as used in the circular spare orbit proposed before, giving an apogee of 500 km. In this case, at 85° for example, the gain is 6 min over 880 hours, that is to say negligible... In fact the best solution is only to decrease a and choose the lowest possible circular orbit to increase $|\dot{\Omega}|$.

Note about Hohmann maneuvers

As the satellite performs continuous thrust, the duration of the burns to commute from the nominal orbit to the phasing orbit need to be computed and added to obtain the total time to replace a failed satellite. The duration of the maneuver is estimated thanks to the Gauss formula of the evolution of the semi-major axis in the case of circular orbits : $\frac{\Delta a}{\Delta t} = \frac{2}{n} T_p$, where a is the semi major-axis, n the mean motion and T_p the acceleration along the velocity. Moreover, Newton's law provides : $T_p = \frac{F}{m}$, with F the thrust and m the total mass of the satellite. For a given thrust F , the duration of the transfer can be estimated by $\frac{nm\Delta a}{2F}$.

During the transfer the semi-major axis of the satellite maneuvering (let us call it the chaser) changes. Therefore the phase gained during the continuous maneuver needs to be taken into account. Let us denote by target the fictitious satellite at the position that need to be reached by the chaser : the situation is the same as a rendezvous with the target orbit the nominal orbit we want to reach. One can write the equality of phase :

$$w_t T + \Delta\theta = w_{ph} T_{ph} + \int_0^{T_m} w_c(t) dt$$

$$T = T_m + T_{ph}$$

With w_t the target mean motion, $w_c(t)$ the chaser mean motion, that depends on the time, w_{ph} the mean motion of the chaser during the phasing if there is one. T is the total duration of the maneuver, T_m is the duration of the two continuous maneuvers (one to go to the phasing orbit and one to go back) and T_{ph} is the duration of the phasing between

the two continuous maneuvers. One can better describe the integral term :

$$\int_0^{T_m} w_c(t) dt = 2 \int_0^{T_m/2} \sqrt{\frac{\mu}{(a_t \pm \frac{t}{T_m/2} d)^3}} dt$$

For simplicity only the case where the phasing orbit is lower than the target orbit is considered (the reasoning is similar and there is no great difference in the maneuver duration obtained at the end). The distance d is the difference between the phasing orbit and the target orbit and a_t is the semi-major axis of the target orbit.

$$\begin{aligned} \int_0^{T_m} w_c(t) dt &= 2 \int_0^{T_m/2} \sqrt{\frac{\mu}{(a_t - \frac{t}{T_m/2} d)^3}} dt \\ \int_0^{T_m} w_c(t) dt &= \frac{2T_m \sqrt{\mu}}{d} \left(\frac{1}{\sqrt{a_t - d}} - \frac{1}{\sqrt{a_t}} \right) \end{aligned}$$

In order to reduce the total time of the maneuvers, one can try to choose T_m and d such that $T_{ph}=0$. T_m is estimated (the mean motion w_t is assumed to not vary a lot) by the Gauss formula $T_m = \frac{nm\Delta a}{F} = \frac{w_t m d}{F}$, giving :

$$\frac{w_t^2 m d}{F} + \Delta\theta = \frac{2w_t m \sqrt{\mu}}{F} \left(\frac{1}{\sqrt{a_t - d}} - \frac{1}{\sqrt{a_t}} \right)$$

The thrust F is supposed to be equal to the drag to decrease the semi-major axis (so it depends on the altitude) and the thrust to increase the semi-major axis is equal to twice the drag at the lowest altitude minus the drag at the current altitude. The mass used for the satellite is 70kg and the data for the drag comes from the study Figure 16a at the worst case.

The results are described table 18. The best strategy seems to be to use only the drag to decrease the semi-major axis (no cost and the service is maintained), and use twice the nominal thrust at least to increase the semi-major axis (cost twice nominal drag compensation and the service might be provided with less power). Notice that no overturn is required, the antennas are still pointing correctly.

| | | | | | | |
|-----------------------------------|------|------|------|------|------|-----|
| Nominal altitude (km) | 350 | 360 | 370 | 380 | 390 | 400 |
| Total maneuver duration (day) | 3.20 | 3.24 | 3.37 | 3.54 | 3.75 | 4 |
| Distance of phasing orbit d (m) | 557 | 547 | 529 | 502 | 474 | 444 |

Table 18: Duration for the replacement of a satellite with continuous thrust (for 1.125° of phase difference to catch with)

| | Phase lag (nominal > phasing) | Phase lead (nominal < phasing) |
|--------------------|--|---|
| Nominal to Phasing | No thrust (drag only) Service can be maintained | Twice max nominal thrust Deteriorated service may be maintained |
| | 180° turn, nominal thrust Service cannot be maintained | |
| Phasing to Nominal | Twice max nominal thrust Deteriorated service may be maintained | No thrust (drag only) Service can be maintained 180° turn, nominal thrust Service cannot be maintained |

Table 19: Strategies for the replacement of a satellite

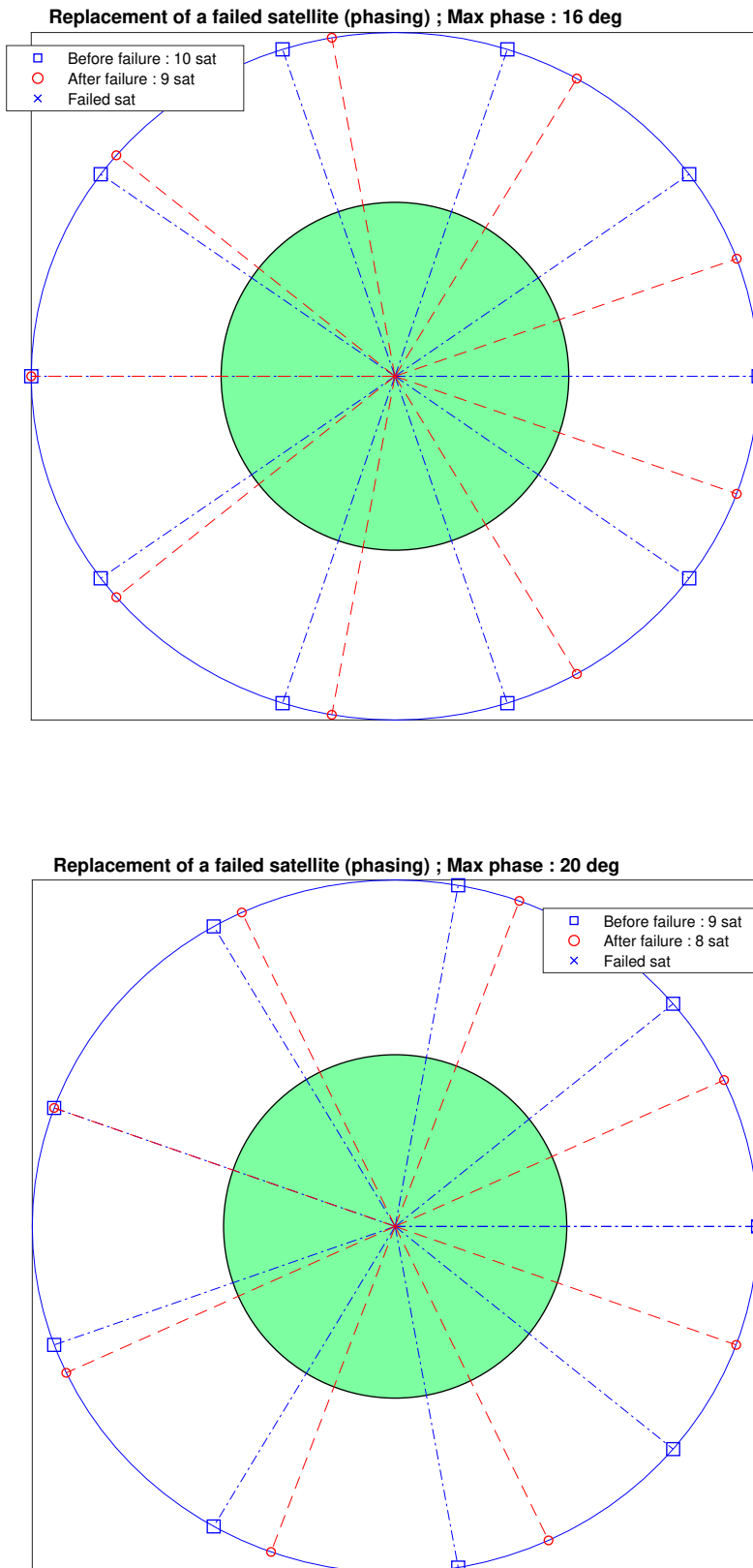


Figure 56: Visualisation of the configuration before a failure and after the failure and phasing (one satellite is dead and not replaced, the configuration evolves from the blue square one to the red circle one). The initial number of satellites per plane here is reduced to 9 and 10 to simplify and cover the odd and even cases.

Phasing maneuver duration with respect to phasing orbit altitude

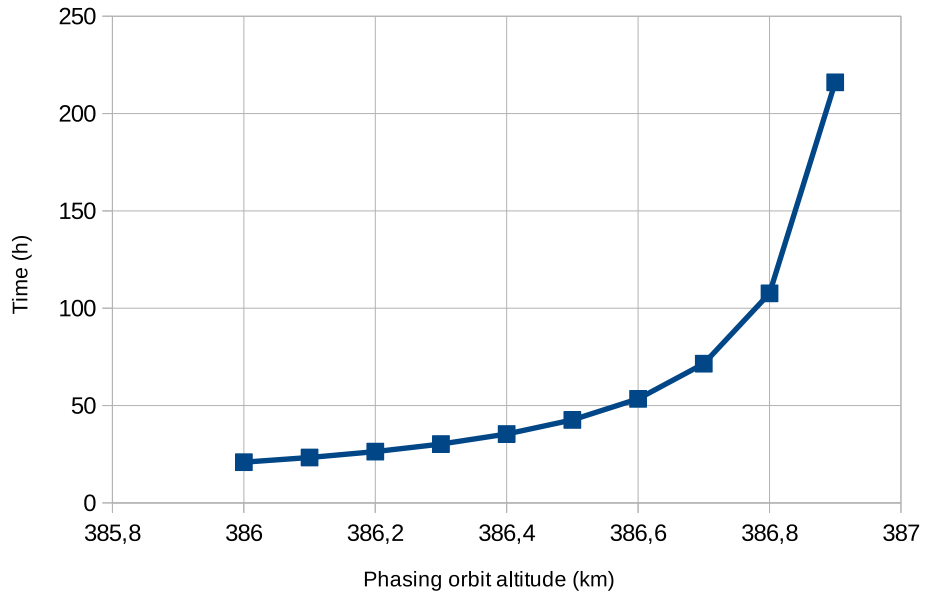


Figure 57: Duration of the phasing maneuver for a switch from 160 to 159 satellites (worst phase to catch up is 1.125°), nominal altitude is 387 km (the highest one giving the worst case) (Two impulsive Hohmann maneuvers case)

Phasing cost with respect to phasing orbit altitude

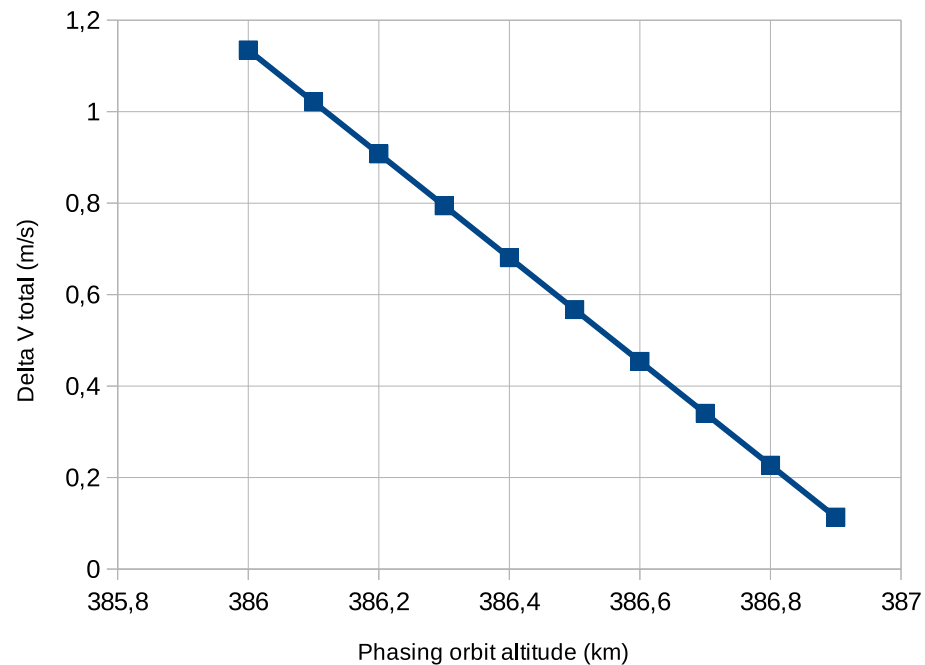


Figure 58: Cost associated to the phasing maneuver (Two Hohmann transfers)

Phasing time to replace one failure vs number of idle satellites

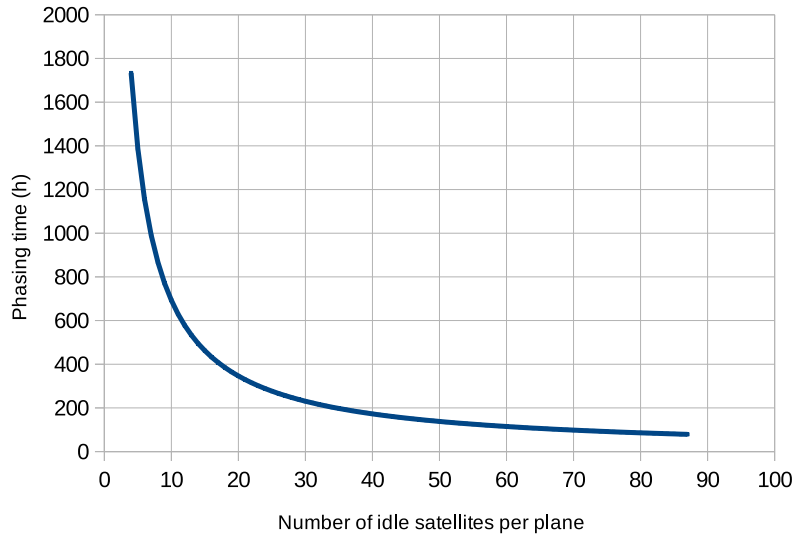


Figure 59: Time for the replacement of one satellite with respect to the number of idle satellites per plane for the first idle spare strategy (Two impulsive Hohmann maneuvers case)

Phasing maneuver duration with respect to phasing orbit altitude

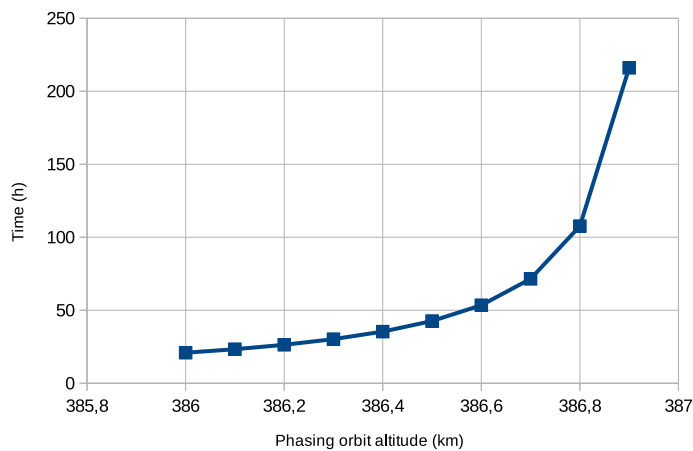


Figure 60: Phasing maneuver depending on the initial phase difference (Two impulsive Hohmann maneuvers case)

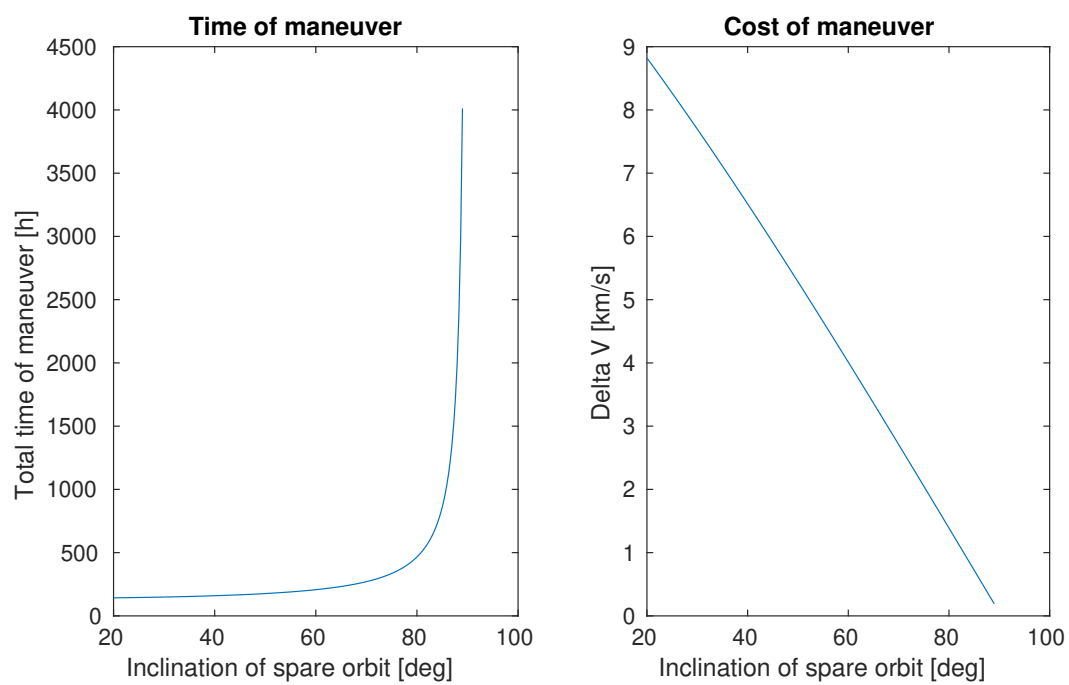


Figure 61: Time and cost of maneuver from the spare orbit to the final position (impulsive Hohmann maneuvers case)

5.5 ADCS concept

Environment and internal torques analysis

The four main sources of torques are gravity-gradient, solar radiation, magnetic field and aerodynamic torque. As the spacecraft is Earth oriented and not inertially oriented, the gravity gradient and aerodynamic torques are constant, however the solar radiation and magnetic field torque are cyclic. All the formulas used here are taken from [1], the details of the formulas can be found in annexe 5.5.

| Torque | Order of magnitude | Formula (from [1] p366) |
|------------------|--------------------------|---|
| Gravity gradient | 3.9×10^{-6} Nm | $\frac{3\mu}{2R^3} I_z - I_x \sin(2\theta)$ |
| Solar radiation | 2.2×10^{-6} Nm | $\frac{F_s}{c} A_s (1+q) (c_{ps} - c_g)$ |
| Magnetic field | 5.25×10^{-5} Nm | $DB \simeq \frac{2DM_0}{R^3}$ |
| Aerodynamic | 9.2×10^{-5} Nm | $0.5\rho C_d AV^2 (c_{pa} - c_g)$ |
| Thrust related | 1×10^{-4} Nm | $ \vec{GC} \wedge \vec{T} $ |

Table 20: Order of magnitude of torques

In the gravity gradient torque, $\mu=3.986 \times 10^{14} \text{ m}^3/\text{s}^2$ and I_z and I_x are the moments of inertia. Here the moments of inertia are considered for the worst case, that is to say the maximum $|I_z - I_x|$. Indeed the spacecraft shape is close to a cylinder with its height along the x axis of the orbital frame, so $I_z \simeq I_y \gg I_x$. With a radius of 30 cm and a length of 1 m and a mass of 100 kg, $I_z \simeq 4.5 \text{ kg m}^2$ and $I_x \simeq 10.5 \text{ kg m}^2$. The distance $R = 6378+350$ km, and we can consider a deviation of the z axis from local vertical $\theta = 10^\circ$.

For the solar radiation torque, the reflectance factor $q = 0.6$ (ranging from 0 to 1), F_s is the solar constant 1367 W/m^2 , c is the speed of light ($3 \times 10^8 \text{ m/s}$), A_s is the surface area (solar panels and satellite body exposed) and $(c_{ps} - c_g)$ is the lever. Let us assume that the lever is 0.1 m.

In the magnetic field torque formula, D is the residual dipole of the vehicle and B the Earth's magnetic field which can be approximated by $\frac{2M_0}{R^3}$ where $M_0=8 \times 10^{15} \text{ T/m}^3$. Typically, the residual dipole of the vehicle D is around 1 Am^2 [1].

In the aerodynamic torque, A is the surface area (solar panels exposed and satellite body), V the spacecraft velocity ($\simeq 7.7 \text{ km/s}$), ρ the atmospheric density (around 10^{-11} kg/m^3), C_d the drag coefficient (around 2.2), $(c_{pa} - c_g)$ is the lever, let us take 0.1 m.

The most important torque to be considered is generated by the misalignment of the thrusters. Indeed, one can consider a 5° cone for the thrust vector and that the center of gravity is located in a box around the geometrical center of the satellite body. In order to compensate the drag due to the atmosphere at 350 km, the maximum thrust is 1.06 mN (see propulsion section). With the knowledge of the center of gravity inside a 5 cm box around the geometrical center of the satellite body, the maximum torque value can be estimated to 1×10^{-4} Nm.

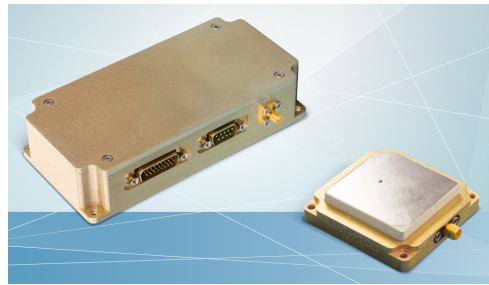


Figure 62: GNSS receiver and antenna

GNSS receiver

The GNSS receiver will help to obtain the position and velocity of the satellite as it will always be in low Earth orbit. The device will help with orbit determination, onboard time synchronization and onboard attitude determination.

The selected GNSS receiver is the NGPS-03-422 from NewSpace Systems with the antenna NANT-PTCL1. The position accuracy is less than 10 m and velocity accuracy is less than 25 cm/s.

The COTS chipset utilised in the NewSpace GPS Receiver has been flying for more than a decade and fifteen flight model units have been built and delivered for launch : the component has flight heritage.

Star trackers

The star tracker provided by Sodern, Auriga, is selected to be used for the mission. This star tracker has a simple architecture using validated COTS with flight proven software. Moreover it was specifically designed for the emerging satellites constellations market. It is designed for at least 7 years, hence it is enough for our mission (the lifetime of the satellites should be around 5 years). Notice that there are two options for the star tracker, either the star tracker is "smart" and provides directly the attitude quaternion or the star tracker only provides the position and magnitude of the stars. In the last case, an additional computing component need to be added.

However one must bear in mind that the star tracker will provide the attitude quaternion only if it does not see the Sun. The Sun exclusion angle is 35° . Two star trackers are enough to ensure attitude estimation all the time. Both devices need to be mounted on the zenith side of the spacecraft (or at least pointing towards the sky) and each pointing direction needs to be separated by at least 70° to be sure that if one star tracker is blinded by the Sun the other one will not be blinded too. By mounting the devices on the zenith side of the spacecraft, they should not see the Earth if the attitude is correctly maintained.

During the mission mode, when the attitude is controlled (nadir-pointing), the angle between the Sun and the pointing direction of the star tracker can be computed. The attitude of the spacecraft is assumed to be nadir pointing and each star tracker is pointing at $\pm 45^\circ$ from zenith (the angle between the two directions is therefore 90°).

Depending on the time of the year and the RAAN of the orbit (the orbit is circular with an inclination fixed to 90°), the angle Sun - star tracker is either near 90° (the orbital plane is perpendicular to the Earth-Sun direction) or it varies from 0° (directly facing the Sun) to 180° (the Sun is directly behind the device) corresponding to the case where the Sun is contain in the orbital plane, Figure 63.

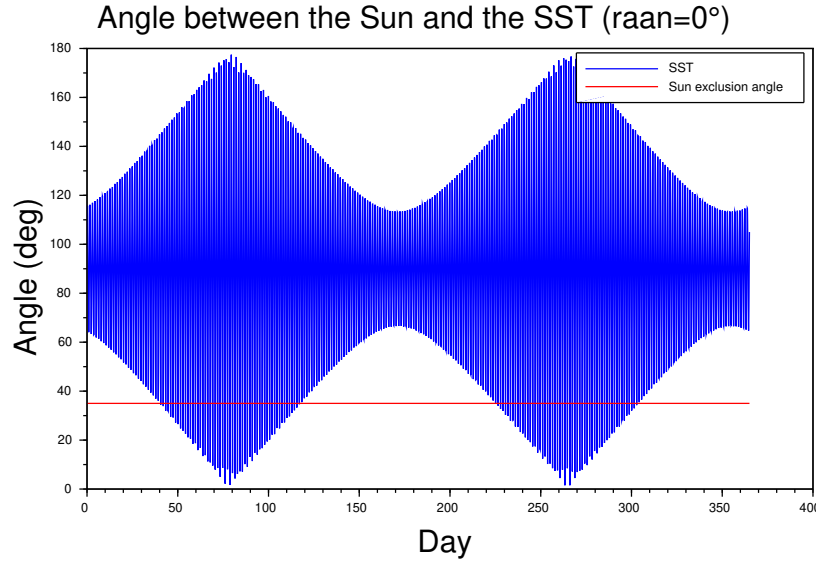


Figure 63: Star tracker angle with respect to the Sun during one year ($\text{RAAN}=0^\circ$), 35° is the sun exclusion angle (similar results are obtained with both star trackers)

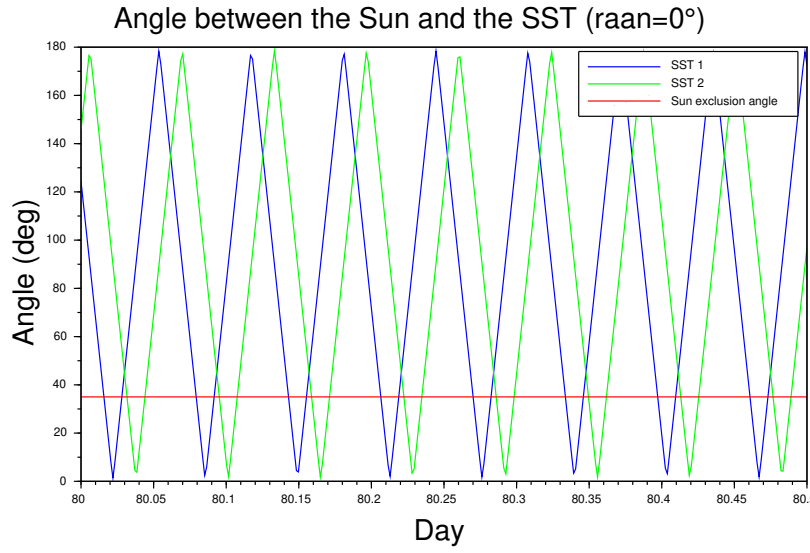


Figure 64: Star tracker 1 and 2 angle with respect to the Sun during the most important blindness period of the year (around day 80 for a RAAN of 0°), 35° is the sun exclusion angle

The star tracker blinding period lasts 80 days and happens twice a year. At 350 km of altitude there are around 16 orbits per day (15.73 exactly), and each day the star tracker is blind during 15 min on average (the maximum is 30 min). So one can estimate the

duration of blindness of the star tracker to $80*2*15*16$, which corresponds to 7% of the year. One can notice that both star trackers will be blinded during different time periods (Figure 64), therefore at least one star tracker is able to estimate the attitude at a given time. However the transition from one star tracker to the other might be fairly short when the Sun is contained in the orbital plane (around 4 min at minimum), therefore a gyroscope would be well suited to propagate the attitude during this switch in order to provide a proper attitude estimate. Notice that in theory the time from lost-in-space @EOL $0.06^\circ/\text{s}$, @99% is less than 11s, and with circular orbits beginning at 350km, the fastest rotation rate that we have is $0.065^\circ/\text{s}$, even with a good margin, it is possible to use only two star trackers. The use of a gyroscope is therefore "optional" during mission mode where the spacecraft is correctly pointing towards nadir. Moreover such a choice would increase the complexity and cost of the system. As the use of two star trackers seems to be enough for the normal mode and the use of sun sensors and magnetometer should be enough for the safe mode, it was chosen to not use a gyroscope.

Magnetometer

The selected magnetometer NMRM-001-485 made by NewSpace Systems. The magnetometer will be used for the calculation of magnetorquer rods control torque levels and also as an additional attitude determination sensor when used with an IGRF reference model.

It has an orthogonality of less than 1 degree, a measurement range of $\pm 60000 \text{ nT}$ and a resolution of 8 nT with a maximum update rate at 18 Hz.

Sun sensors



Figure 65: Coarse Sun Sensor provided by Space Micro

The use of a few sun sensors will help to locate the Sun during safe mode or during critical phases when the solar arrays should be pointed towards the Sun to acquire a maximum of power.

The coarse sun sensor selected is provided by Space Micro, figure 65. This coarse sun sensor contains a single photodiode, with the housing assembly also serving as an aperture. The inexpensive, lightweight sensor (only 20g) draws no power and has an accuracy of better than ± 5 degrees over a full angle 120 degree field of view.

Three to four sun sensors can be used : three positioned at 120° on the cylinder and one in the front face (velocity face). Such configuration allows to determine the position of the Sun if it is around the satellite body or aligned with the body in front of the satellite,

however if the Sun is exactly behind the spacecraft body, it will not be possible to obtain precisely its position.

The choice to not put an extra sensor on the back face is motivated by the fact that the device might not perform correctly due to the plume of the thrusters.

Reaction wheels

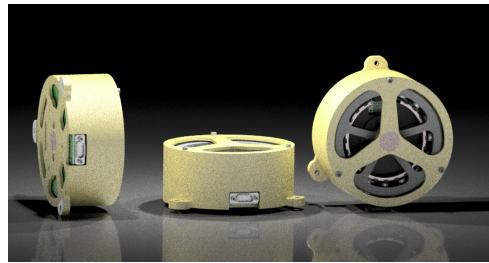


Figure 66: Reaction wheel from Sinclair Interplanetary (400 mNms momentum)

The most important torque is the one generated by the thruster misalignment (within a 5° cone), the maximum thrust value is 1.06 mN with the knowledge of the center of gravity in a 5 cm box : therefore the torque generated by the reaction wheels should be able to generate at least 0.1 mN.m of torque (value obtained by computing the torque with a random orientation of the thrust within the 5° cone and a random center of gravity inside the 5 cm box). The issue is that this torque is constant as it is required to compensate the drag constantly.

One idea might be to off load the wheels when the satellite is above $\pm 70^\circ$ of latitude, relaxing the pointing accuracy needed for the mission as it considered that there is no business at these high latitudes. During the orbits above the sea, a full off loading might also be performed.

Using this as a sizing rule, the reaction wheel need to provide 0.1 mN.m during $70*2/360*100=39\%$ percent of an orbit, that is to say around 2160 s. The momentum that need to be stored at maximum is therefore 0.2 N.m.s (0.0001 N.m * 2160 s). When the satellite is higher than $\pm 70^\circ$ of latitude, a regenerative braking can be performed, the reaction wheels are giving back some energy and are off loaded thanks to the magnetorquers.

Therefore a reaction wheel with momentum storage of 0.2 N.m.s and a maximum torque of at least 0.1 mN.m should fit the purpose here.

With some estimations with existing reaction wheels, the closest product is provided by Sinclair Interplanetary with a 400 mNms Microsatellite Wheel (light rotor) Figure 66, suitable for microsatellites. These reaction wheels have a strong flight heritage, with 52 units on-orbit. These wheels can provide a torque up to ± 100 mNm which is clearly oversized for our application, hence an improvement might be done by the manufacturer to obtain a product fitted to the mission. However such data helps to obtain an estimate of the size and mass of one reaction wheel. Its mass should be around 500 g and dimensions around 100 mm of diameter and 48 mm of height. Notice that this first sizing is quite rough and probably oversizing the needs : a proper simulation should be performed to

better estimate the reaction wheels characteristics. Such wheel is supplied by 28 V, and according to the power consumption of this kind of reaction wheel, for the scenario of a completely off loaded wheel at -70° of latitude to $+70^\circ$ with a constant torque at 0.1 mN.m, the power consumption goes linearly from 0 W to $0.4 \times 28 \approx 11$ W. The main characteristics of the reaction wheel design can be found table 21.

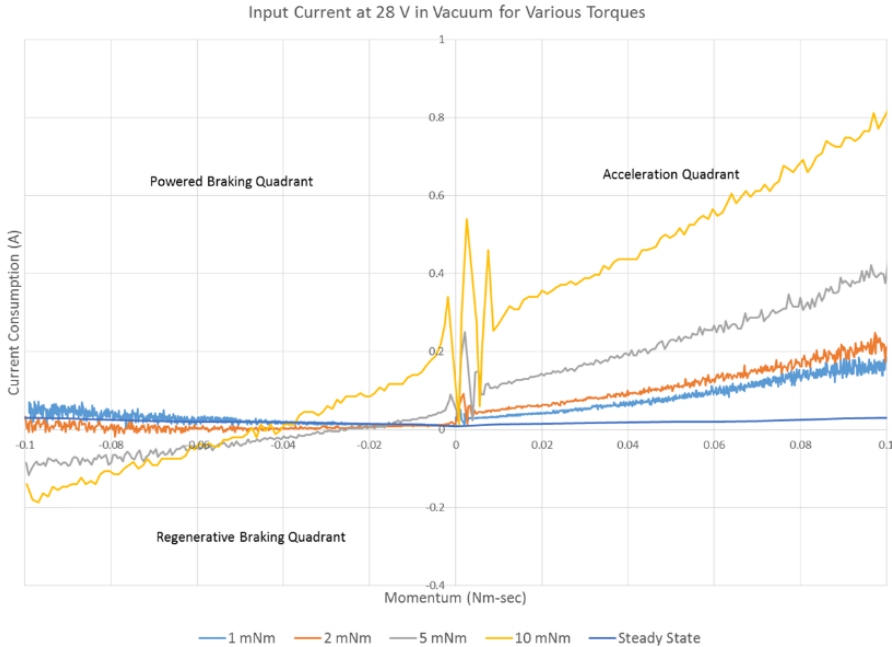


Figure 67: Consumption of the Microsatellite Reaction Wheels (RW3-0.06) from Sinclair Interplanetary

| Momentum storage | Maximum torque | Mass | Size | Power |
|------------------|----------------|-------|-------------------------------|------------|
| 0.2 N.m.s | >0.1 mN.m | 500 g | 100 mm diameter, 48 mm height | cf Fig. 67 |

Table 21: Reaction wheel design

Magnetorquers

The main goal of the magnetorquers will be to off load the reaction wheels and also to detumble the satellite just after the launch. Three rods will be used along each axis x, y and z of the satellite body.

Some typical characteristics of magnetorquers are provided 22. According to the datasheet of the iMTQ by ISIS, such device with three magnetometers is designed for a 24 kg cubesat, whereas the rod used for the PROTEUS platform is designed for 500 kg satellites, which would clearly be over-designed for our case. The rods from NewSpace Systems give a interesting data range to perform extrapolation for the sizing of the magnetorquers.

Most of the magnetorquers found on the market are easily customizable, therefore the provider does not seem to be a huge constraint.

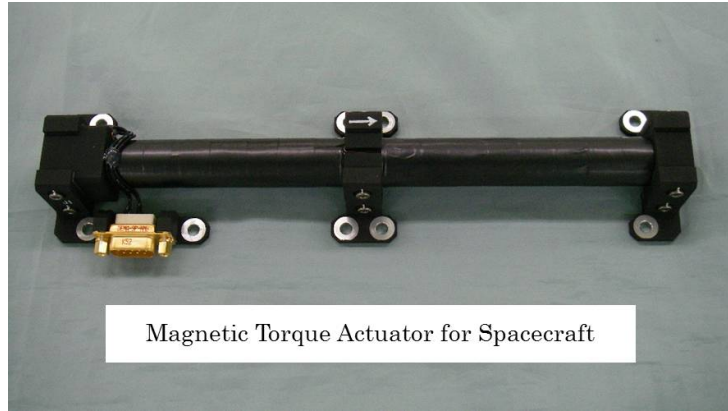


Figure 68: Magnetorquer rod from Meisei Electric

| Supplier/satellite | Mag. moment | Mass | Size | Power |
|--------------------|-----------------------|---------------|----------------------|-------|
| iMTQ (ISIS) | 0.2 Am ² | 196g | 95.9x90.1x17 mm | 1 W |
| NewSpace Systems | 1-100 Am ² | 55g/cm length | Φ12 mm,L=80-600 mm | >1 W |
| Meisei Electric | 12 Am ² | 500 g | 56x29x250 mm (rod) | 1 W |
| PROTEUS | 60 Am ² | 1.7 kg | Φ26mm,L=640 mm (rod) | 6 W |

Table 22: ADCS architecture and modes

The magnetorquers required for the mission need to generate at least the same torque as the reaction wheel to be able to desaturate them correctly. The torque generated by a magnetorquer rod is equal to the magnetic field of the Earth times the magnetic dipole of the magnetorquer. The Earth magnetic field can be represented in a first approximation by the formula :

$$|B| = \frac{B_0}{R^3} \sqrt{1 + 3\sin(\lambda)^2}$$

As the maximum momentum stored by the reaction wheels is 0.2 N.m.s, the magnetorquers need to generate a torque of 0.3 mN.m to off load 0.2 N.m.s during 20*2/360*100 percent of the orbit. Therefore thanks to the value of the magnetic field in the worst case ($\lambda=0$, hence $2.6 \cdot 10^{-5}$ T), the magnetic dipole should be equal to $\frac{0.2 \cdot 10^{-3}}{2.6 \cdot 10^{-5}} = 12 A.m^2$. The dimensions and mass of the magnetorquer can be estimated thanks to the values provided by the manufacturer NewSpace Systems. A length of 85 mm with a 12 mm diameter is obtained, giving a mass of 470 g. The power consumption can be estimated around 3 W according to the existing technologies. A sum up of the magnetorquer design can be found in table 23. Notice that this first sizing is quite rough and probably oversizing the needs : a proper simulation should be performed to better estimate the magnetorquer characteristics.

| Magnetic moment | Mass | Size | Power |
|--------------------|------|-----------------------|-------|
| 12 Am ² | 470 | Φ=12 mm, length=85 mm | 3 W |

Table 23: Magnetorquer design

Power consumption over one orbit

As the orbit have a 90° inclination, one can consider the position on orbit with respect to its current latitude, here from -70° to 90° the pole (the business area is covered between ±70°). The situation is symmetrical for the rest of the orbit. Between -70° and 70°, the magnetorquers are off and the reaction wheels are speeding to generate a torque of 0.1 mN.m (worst case estimate due to the thrust misalignment). According to the reaction wheel datasheet 67 of the reaction wheel closest to the characteristics found, the required power goes from 0 W to 11 W at the maximum at 70° of latitude for the set of three reaction wheels. Then the desaturation phase begins after 70°, the magnetorquers are powered to compensate the torque lost by the reaction wheels that are braking. Moreover the braking of the reaction wheels is regenerative, therefore some power can be recovered during the operation.

Detumbling

With the choice of the magnetorquer rods, a simulation is performed with a tool developed at ISAE-Supaero during several student projects called PILIA, which is a general tool for development and validation of the Attitude and Orbit Control System. The tool is also able to perform rendez-vous and orbital maneuvers simulations. With the characteristics of the satellite and the magnetorquer rods, and a B-dot control, which is basically applying the following torque :

$$\vec{M}_{com} = -\frac{k}{||\vec{B}||}\dot{\vec{b}}$$

where \vec{B} is the local Earth's magnetic field, expressed in the satellite frame of reference, and $\dot{\vec{b}}$ is the time derivative of the unit vector defining the direction of the local Earth's magnetic field, in the satellite reference frame. k is the gain of the controller, chosen to be equal to the maximum moment of inertia of the satellite divided by the time constant 1000 s.

The simulation Figure 69 shows that the detumbling with only the magnetorquers and a B-dot law is enough to stabilise the satellite from an initial random tumbling rate of 3° per second. In less than half an orbit the satellite is stabilised.

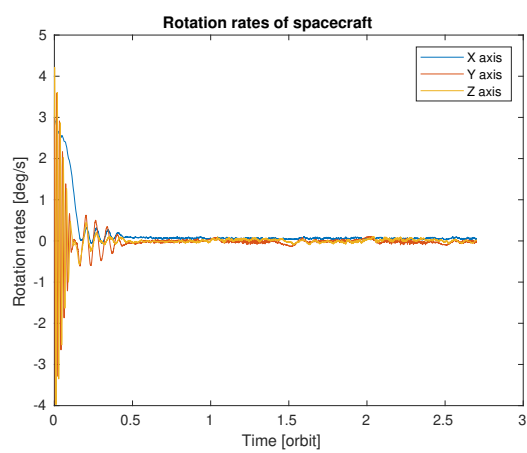


Figure 69: Worst case power consumption estimate for the actuators

References

- [1] WJ Larson and JR Wertz. Space mission analysis and design third edition. *Space Technology Series*, 8, 1999.
- [2] Teruhisa Sugimoto and Masaharu Tanemura. Random sequential covering of a sphere with identical spherical caps. *FORMA-TOKYO-*, 16(3):209–212, 2001.
- [3] James Richard Wertz. Mission geometry: orbit and constellation design and management: spacecraft orbit and attitude systems. *Mission geometry: orbit and constellation design and management: spacecraft orbit and attitude systems/James R. Wertz. El Segundo, CA; Boston: Microcosm: Kluwer Academic Publishers, 2001. Space technology library; 13*, 2001.
- [4] Thomas Wolf and Jean-Jacques De Ridder. Resistance to satellite failures of leo communication systems. 1992.